

SEISMIC EVALUATION AND RECONNAISSANCE TDEM SURVEY OF THE SOUTHEAST  
AND PLAYA 3 AREAS OF THE PANTEX PLANT, CARSON COUNTY, TEXAS

by

Jeffrey G. Paine

prepared for

Sandia National Laboratories  
Innovative Treatment Remediation Demonstration Program  
P.O. No. 12236

Bureau of Economic Geology  
Scott W. Tinker, Director  
The University of Texas at Austin  
Austin, Texas 78713-8924

October 2000

## CONTENTS

ABSTRACT .....	1
INTRODUCTION .....	4
FINE-GRAINED-ZONE PROPERTIES AND APPLICABLE NONINVASIVE METHODS .....	4
EXISTING SEISMIC DATA .....	5
RECONNAISSANCE TDEM SURVEY .....	11
Modeling Results .....	16
Signal Adequacy .....	22
Pantex Southeast Results .....	25
Playa 3 Area Results .....	40
SEISMIC REFLECTION SUMMARY AND RECOMMENDATIONS .....	43
TDEM SUMMARY AND RECOMMENDATIONS .....	47
ACKNOWLEDGMENTS .....	49
REFERENCES .....	49

## FIGURES

1. Map of the Pantex Plant showing the location of seismic reflection lines acquired by Ebasco Services Incorporated for the U.S. Army Corps of Engineers .....	7
2. Sample interpreted seismic section from line 1 of the seismic reflection survey acquired by Ebasco Services Incorporated for the U.S. Army Corps of Engineers .....	8
3. Location of playa and interplaya seismic reflection lines acquired by the Bureau of Economic Geology in the vicinity of the Pantex Plant .....	9
4. TDEM transmitter input and receiver response .....	12
5. Reconnaissance TDEM sounding sites and nearby water wells in the southeast part of the Pantex Plant .....	13
6. Reconnaissance TDEM sounding sites and nearby water wells in the Playa 3 and Burning Grounds area of the Pantex Plant .....	14
7. Central loop instrument configuration for TDEM soundings at the Pantex Plant .....	17
8. Resistivity log and generalized resistivity model for well BEG-PTX2 in the southwest part of the Pantex Plant .....	19

9.	Predicted transient signal for the generalized resistivity model from well BEG-PTX2 .....	20
10.	Predicted apparent resistivity curves for the generalized resistivity model from well BEG-PTX2 .....	21
11.	Predicted transient signal for the generalized resistivity model from well BEG-PTX2 assuming a transmitter loop current of 18 amperes and loop sizes ranging from 40 × 40 m to 120 × 120 m .....	23
12.	Comparison of actual transient recorded at site TDEM 4 with the transients predicted for the generalized resistivity models .....	24
13.	Comparison of transient signal with background noise for z-axis data at site TDEM 7 in the Pantex Southeast area .....	26
14.	Comparison of transient signal with background noise for z-axis data at site TDEM 8 in the Playa 3 area .....	27
15.	Comparison of z-axis transient with x- and y-axis transients at site TDEM 9 in the Playa 3 area .....	28
16.	Comparison of z-axis transient with x- and y-axis transients at site TDEM 4 in the Pantex Southeast area .....	29
17.	Transients recorded at sites TDEM 4, 3, and 1 along a west–east series in the Pantex Southeast area .....	31
18.	Transients recorded at sites TDEM 1, 6, 5, 7, and 10 along a south–north series in the Pantex Southeast area .....	32
19.	Apparent resistivity curves calculated for transients recorded at sites TDEM 4, 3, and 1 along a west–east series in the Pantex Southeast area .....	33
20.	Apparent resistivity curves calculated for transients recorded at sites TDEM 1, 6, 5, 7, and 10 along a south–north series in the Pantex Southeast area .....	34
21.	Apparent resistivity data recorded at site TDEM 1 and the synthetic apparent resistivity curves calculated from best-fit and equivalent-fit resistivity models .....	36
22.	Three-layer resistivity models that fit transients recorded at sites TDEM 4, 3, and 1 in the Pantex Southeast area .....	38
23.	Two- to four-layer resistivity models that fit transients recorded at sites TDEM 1, 6, 5, 7, and 10 in the Pantex Southeast area .....	39
24.	Transients recorded at sites TDEM 2, 8, and 9 in the Playa 3 area .....	41
25.	Apparent resistivity curves calculated for transients recorded at sites TDEM 2, 8, and 9 in the Playa 3 area .....	42
26.	Three- to five-layer resistivity models that fit transients recorded at sites TDEM 2, 8, and 9 in the Playa 3 area .....	44

## TABLES

1. Location and elevation of TDEM soundings acquired in the southeast and Playa 3 areas of the Pantex Plant, September 18–22, 2000 .....	15
2. Best-fit models for TDEM soundings in the Pantex Southeast area .....	37
3. Best-fit models for TDEM soundings in the Playa 3 area .....	45

## ABSTRACT

In response to a recommendation in the recent “Protecting the Ogallala Aquifer II” report, the Bureau of Economic Geology (the Bureau) evaluated the potential of seismic reflection and TDEM methods to define the distribution and thickness variations of the Ogallala fine-grained zone (FGZ) that perches ground water beneath the Pantex Plant. Bureau researchers briefly examined existing seismic reflection data collected at and near the Pantex Plant by the U.S. Army Corps of Engineers (COE) and by the Bureau, conducted TDEM modeling studies, and acquired reconnaissance TDEM data in the Pantex Southeast and Playa 3 areas.

The existing seismic reflection surveys had broad objectives that extended from the Ogallala caprock to the base of the Ogallala Formation. These surveys provided basic data on the stratigraphic framework of playa and interplaya areas. Although the top of the FGZ appears to be a good seismic reflector in existing data, reprocessing the limited COE and Bureau seismic data in the Pantex Southeast area might enhance that reflection and reveal other associated reflectors in the same depth range. Further improvement in the seismic characterization of the FGZ would require acquisition of new seismic data that would benefit from the restricted target depth and recent advances in seismic equipment.

In the Pantex Southeast area, new data could be acquired along multiple lines to provide better FGZ definition. These data might be expected to detect the presence or absence, the top, and perhaps the base of the FGZ. Three-dimensional seismic data could be acquired over small areas such as Playa 3 and the Burning Grounds. These data would be expected to reveal structural and stratigraphic features that distinguish playa and interplaya environments and influence ground-water migration.

Existing data demonstrate that the resolution that is readily achievable using seismic methods is limited. Under favorable conditions, resolution within the FGZ is limited to reflectors that are more than 4 to 8 m apart. This resolution is sufficient to resolve the top and bottom of the FGZ where it is relatively thick. Seismic shear waves have shorter wavelengths than compres-

sional waves and can achieve higher resolution than is obtained with compressional waves. A survey employing a shear wave source might provide better FGZ resolution.

In the EM method, we exploit the increase in conductivity associated with higher clay and water content to help map the FGZ and estimate its integrity as an aquitard. Our approach to establishing whether TDEM provides useful information was to (a) predict the detectability limits of the TDEM method by modeling the perched aquifer and FGZ and (b) prove the viability of the method by acquiring and comparing TDEM soundings at representative locations at the Pantex Plant.

Modeling showed that the presence or absence and the thickness of the FGZ are theoretically resolvable and that exploration depths greater than that of the FGZ can be achieved. Field measurements showed that the Southeast and Playa 3 areas are low-EM noise environments that satisfy the lateral homogeneity assumption at most sites, allowing resistivity models to be constructed that portray generalized resistivity changes with depth beneath the sites.

TDEM data recorded at 10 reconnaissance sites show differences that are caused by changes in the electrical properties of the subsurface, resulting in different resistivity models that fit the observed data at each site. The TDEM method appears to be unable to resolve the thickness of the FGZ, but the FGZ does appear to strongly influence the TDEM signal and the resulting resistivity models. The northward increase in FGZ thickness in the Pantex Southeast area causes a progressive decrease in resistivity in the model layer at the depth of the FGZ. TDEM data acquired at Playa 3 differ greatly from data acquired outside the playa. The playa floor measurements indicate a higher clay content surface layer that is underlain by coarser or more porous deposits than are present at similar depths outside the playa. EM and seismic reflection data both suggest that strata beneath the playa differ from those in interplaya environments. This is a potential source of error in hydrologic models that assume similar hydraulic properties in these settings.

High-quality TDEM data can be acquired at the Pantex Plant, variation in the resistivity structure is sufficient within both areas studied to detect subsurface change, and the TDEM data

are useful in estimating the intensity of FGZ development and in examining lithologic differences at depth. Reconnaissance TDEM data are too widely spaced to provide the spatial density that would be required to map subtle changes in FGZ thickness, FGZ absence in local areas, or channel features. Future TDEM efforts should be directed toward increasing the spatial density of the measurements by collecting closely spaced soundings along key transects using ground-based equipment or by acquiring data along closely spaced flight lines using airborne equipment. Key areas where additional TDEM data would be useful include areas east and north of the main Pantex Plant zones.

## INTRODUCTION

The “Protecting the Ogallala Aquifer II” report (U.S. Department of Energy Technical Assistance Team, 2000) states that “geophysical methods such as time domain electromagnetic soundings (TDEM) and seismic methods should be considered” to provide information on the areal extent, thickness, and lithologic variability of the perched water aquitard in the southeast plume area. The Bureau of Economic Geology (the Bureau), through a contract with Sandia National Laboratories, evaluated these two methods for potential application in the Pantex Plant area.

During September and October 2000, Bureau researchers briefly examined existing seismic reflection data collected at the Pantex Plant for the U.S. Army Corps of Engineers and by the Bureau at and near the Pantex Plant. Bureau researchers also conducted TDEM modeling studies and acquired reconnaissance TDEM data in the Playa 3 and Pantex Southeast areas to examine the feasibility of this method in understanding the lateral distribution and thickness variations of the Ogallala fine-grained zone (FGZ) that perches ground water in places beneath the Pantex Plant. This report briefly summarizes the key findings of these investigations.

### FINE-GRAINED-ZONE PROPERTIES AND APPLICABLE NONINVASIVE METHODS

Noninvasive geophysical methods that might provide useful information on the Ogallala FGZ are those that sense physical properties that are unique to the FGZ. Proper application of the appropriate methods depends on the depth of the target, its thickness, the approximate value of the measured physical property in the target and the host, and the contrast in the measured physical property between the target and its host.

Numerous borings and wells have reached the Ogallala FGZ during Pantex Plant operation, characterization, and remediation activities. Although it is beyond the scope of this study to examine the FGZ in detail, enough already is known about the gross geometry and physical properties of the FGZ to determine applicable geophysical methods and design appropriate field studies.



Subsurface data indicate that the FGZ is composed of several distinct clay-rich layers within a coarser grained matrix (Gustavson and others, 1995). Electrical logs from Pantex and surrounding wells verify the common observation that high clay content translates to increased electrical conductivity of the sediment. Borehole seismic measurements in an Ogallala monitoring well south of Playa 2 (BEG-PTX2) document an increase in seismic velocity within the FGZ. Further, water-saturated sediment within the perched aquifer most likely has higher density, seismic velocity, and electrical conductivity than similar unsaturated stratigraphic intervals. These observations from existing data suggest that seismic and electrical methods are appropriate tools to investigate the FGZ and associated perched aquifer. Variations in density, sediment type, and water saturation within the perched aquifer and FGZ might be large enough to image using seismic reflection methods, including the top and perhaps the base of the FGZ where it is sufficiently thick. Increases in electrical conductivity caused by water saturation within the perched aquifer and by increased clay content within the FGZ might be detected using electromagnetic induction methods, especially TDEM.

The design and feasibility of appropriate seismic reflection and EM surveys depend upon the depth and thickness of the FGZ and perched aquifer. Using values reported in the groundwater program management action process (U.S. Department of Energy, Amarillo Area Office, 2000), depth to perched water averages 73 m. Saturated thickness averages 4 m, ranging from 0 to about 23 m. The underlying FGZ is reached at an average depth of 78 m. Its thickness is poorly constrained, but existing data suggest an average thickness of about 16 m. Consequently, the depth of interest ranges from about 60 to 120 m; the combined target thickness (FGZ and saturated zone) averages about 20 m.

## EXISTING SEISMIC DATA

Two major seismic reflection surveys have been conducted at and near the Pantex Plant. One survey, in which plant-specific data were acquired, processed, and interpreted by Ebasco

Services Incorporated for the U.S. Army Corps of Engineers (COE), was completed in 1992 and summarized in the COE's Hydrogeological Assessment (U.S. Army Corps of Engineers, 1992). This survey consists of five seismic line segments oriented north–south and eight segments oriented east–west across the Pantex Plant (fig. 1). The total distance surveyed was 28 km. Broad objectives that dictated survey design included targets as shallow as the Ogallala caprock at about 25 m and as deep as the base of the Ogallala at depths of 125 to 250 m. In addition to the interpreted seismic lines, other products based on seismic interpretations included depth to the caprock, depth to the red beds, and thickness of the FGZ. An example of the processed Ebasco seismic data (fig. 2) shows the interpreted expression of the targets of interest, including the Ogallala caprock, the top and bottom of the FGZ, and the top of the red beds (base of the Ogallala).

Known difficulties with interpretations of the Ebasco data include (a) significant discrepancies between interpreted and actual depth to the base of the Ogallala along line 3 (about 120 m in well BEG-PTX2 and about 170 m on line 3) and (b) a general lack of clear reflectors in the processed data, particularly in the middle to lower Ogallala section. These difficulties are related to the fact that, above the Ogallala aquifer, unsaturated sediments propagate high-frequency seismic energy (above about 50 Hz) poorly. The 100-Hz geophones used in the Ebasco survey to enhance the high-frequency response most likely filtered out a significant part of the lower frequency signal that would help investigate the deeper parts of the Ogallala.

The eastern half of Ebasco line A and all of line 2 are located within the Pantex Southeast area (fig. 1). These lines may contain stratigraphic information that might be further analyzed with subsurface data that have been collected in the area since the Ebasco survey was completed. No Ebasco seismic data were acquired near Playa 3.

The Bureau acquired seismic reflection data on and near the Pantex Plant (fig. 3) between 1991 and 1994 (Gustavson and others, 1995). These data included 35 km of reflection data in interplaya settings (Gustavson and others, 1995; Paine, 1992) and more than 15 km of data across playas, including Pantex Playa 3 (Paine, 1994a) and 5 (Paine, 1995a), Pantex Lake

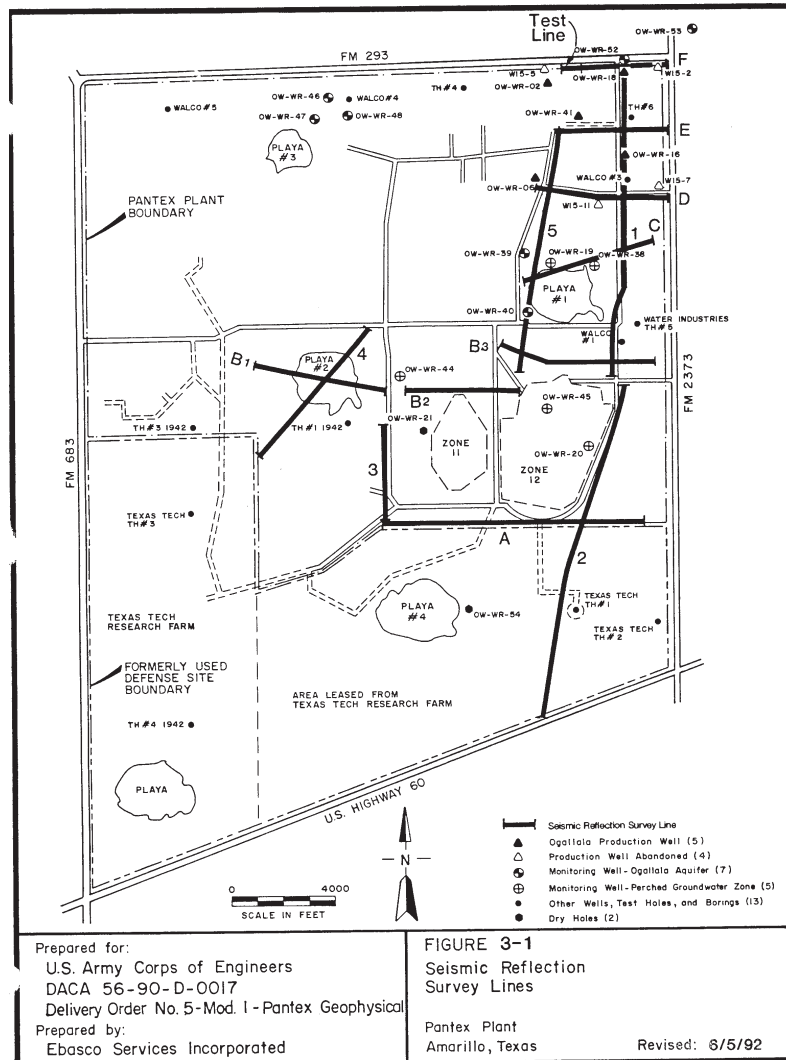


Figure 1. Map of the Pantex Plant showing the location of seismic reflection lines acquired by Ebasco Services Incorporated for the U.S. Army Corps of Engineers (from U.S. Army Corps of Engineers, 1992).

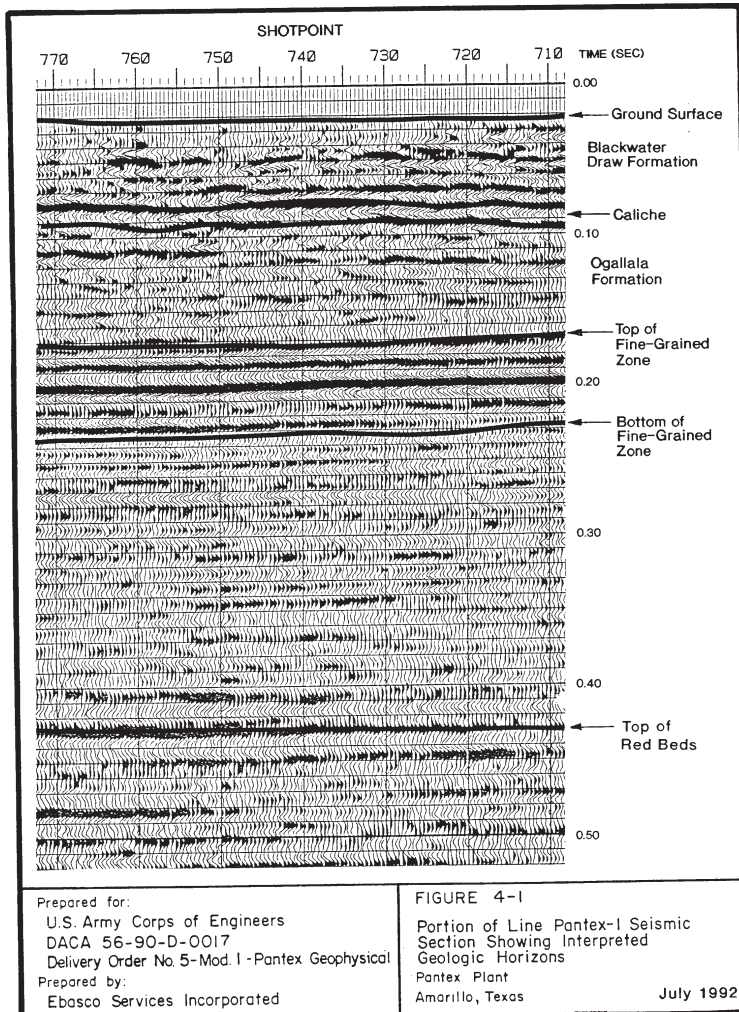


Figure 2. Sample interpreted seismic section from line 1 of the seismic reflection survey acquired by Ebasco Services Incorporated for the U.S. Army Corps of Engineers (from U.S. Army Corps of Engineers, 1992).

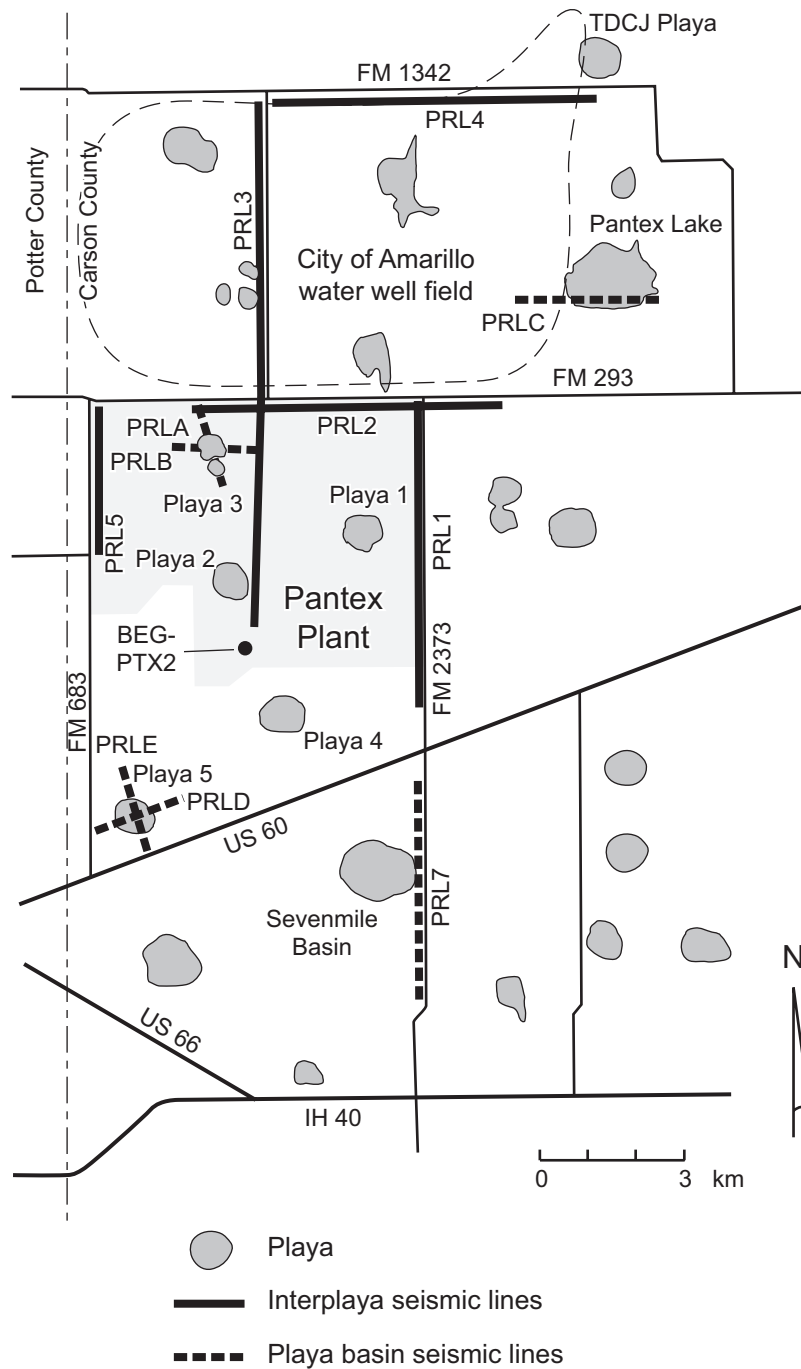


Figure 3. Location of playa and interplaya seismic reflection lines acquired by the Bureau of Economic Geology in the vicinity of the Pantex Plant. Outlined area encloses the City of Amarillo water well field.

(Paine, 1994b), and Sevenmile Basin (Paine, 1993). The surveys were designed to explore to depths of 30 to 250 m using a weight-drop seismic source and an array of 40-Hz geophones. Most of the processing and interpretation effort was focused on lines across playa basins, which represent important recharge paths for the Ogallala, as well as areas where little was known about subsurface stratigraphy. Products from these surveys included seismic images of subsurface reflectors that were interpreted to represent the top of the Ogallala caprock, the top of the middle Ogallala FGZ, and the base of the Ogallala.

Seismic lines acquired by the Bureau across each of the playa basins studied, including Playa 3, have been interpreted to show evidence of subsidence that may be related to subsurface dissolution of Permian evaporites (Paine, 1994c; 1995b). If these interpretations are correct, it is likely that poorly characterized Cenozoic deposits beneath the playa basins differ substantially from better characterized, correlative sediments outside of the playa basins. On the Playa 3 lines, for example, the interpreted caprock reflector is absent beneath the playa, suggesting that the caprock either never formed or has been dissolved by recharging ground water. If the playas are a manifestation of subsurface dissolution and subsidence of overlying strata, then the sediments beneath the playas can be expected to be finer grained to an unknown depth than surrounding sediments, owing to long-term deposition in an ephemeral lake environment, and perhaps be disrupted by dissolution-related subsidence at greater depths. The ground-water flow paths and rates in a stratigraphic section such as this might differ substantially from those beneath well-characterized interplaya areas.

The only Bureau interplaya line in the Pantex Southeast area is the southern part of line 1, which was acquired in 1991 along FM 2373. Major reflectors on this line are interpreted as the middle Ogallala FGZ, a lower Ogallala FGZ, and the top of bedrock (Gustavson and others, 1995). Estimated depths for these reflectors in the Pantex Southeast area are near 75, 120, and 175 m but vary with position along the line. There is some suggestion of broad, thin, channel-shaped features at about the level of the middle Ogallala FGZ, but specialized processing and further analysis would be required to enhance these possible features.

## RECONNAISSANCE TDEM SURVEY

To test the viability of the time-domain electromagnetic induction (TDEM) method in addressing issues related to the perched aquifer at the Pantex Plant, the Bureau performed preliminary modeling and reconnaissance field investigations in the Pantex Southeast and Playa 3 areas. Because the electrical properties change with changes in clay content and water saturation, surface methods that measure subsurface electrical conductivity show promise in detecting changes caused by the presence or absence of the Ogallala FGZ and variations in the thickness of the FGZ and the saturated thickness of the perched aquifer.

The EM family of geophysical methods (Parasnis, 1973; Frischknecht and others, 1991; West and Macnae, 1991) employs a changing primary magnetic field that is created around a current-carrying transmitter wire to induce a current to flow within the ground, which in turn creates a secondary magnetic field that is sensed by a receiver coil. In general, the strength of the secondary field is proportional to the conductivity of the ground. TDEM methods (Kaufman and Keller, 1983; Spies and Frischknecht, 1991) measure the decay of a transient, secondary magnetic field produced by the termination of an alternating primary electric current in the transmitter loop (fig. 4). The secondary field, generated by current induced to flow in the ground, is measured by the receiving coil following transmitter current shutoff. Secondary field, or transient, strength at an early time gives information on conductivity in the shallow subsurface; transient strength at later times is influenced by conductivity at depth.

We acquired seven TDEM soundings in the Pantex Southeast area (fig. 5) and three TDEM soundings in the Playa 3 area (fig. 6) in September 2000. The location of each TDEM sounding was determined by Pantex staff using a GPS receiver (table 1). To select the appropriate survey geometry and acquisition parameters, we conducted modeling studies using the software RECTAN provided by Geonics and induction log data from well BEG-PTX2. For the field studies, our transmitter loop was constructed of a single loop of 12-gauge copper wire that measured  $100 \times 100$  m. At each site, we placed the receiver coil in the center of the transmitter

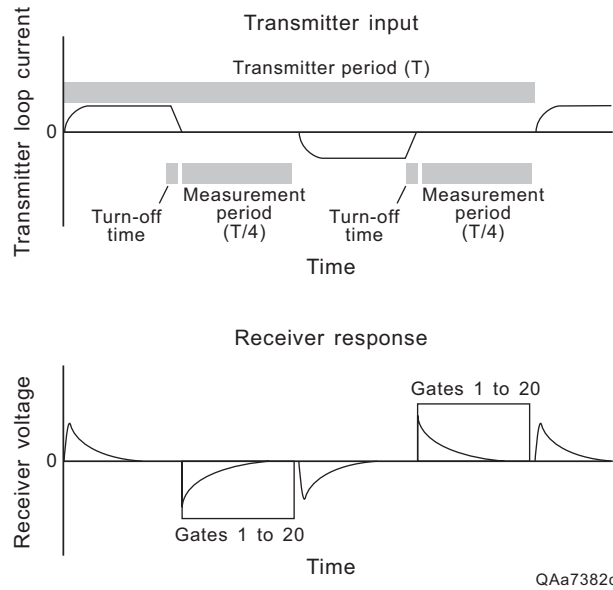


Figure 4. TDEM transmitter input (upper graphic) and receiver response (lower graphic). Adapted from Geonics Limited (1992).



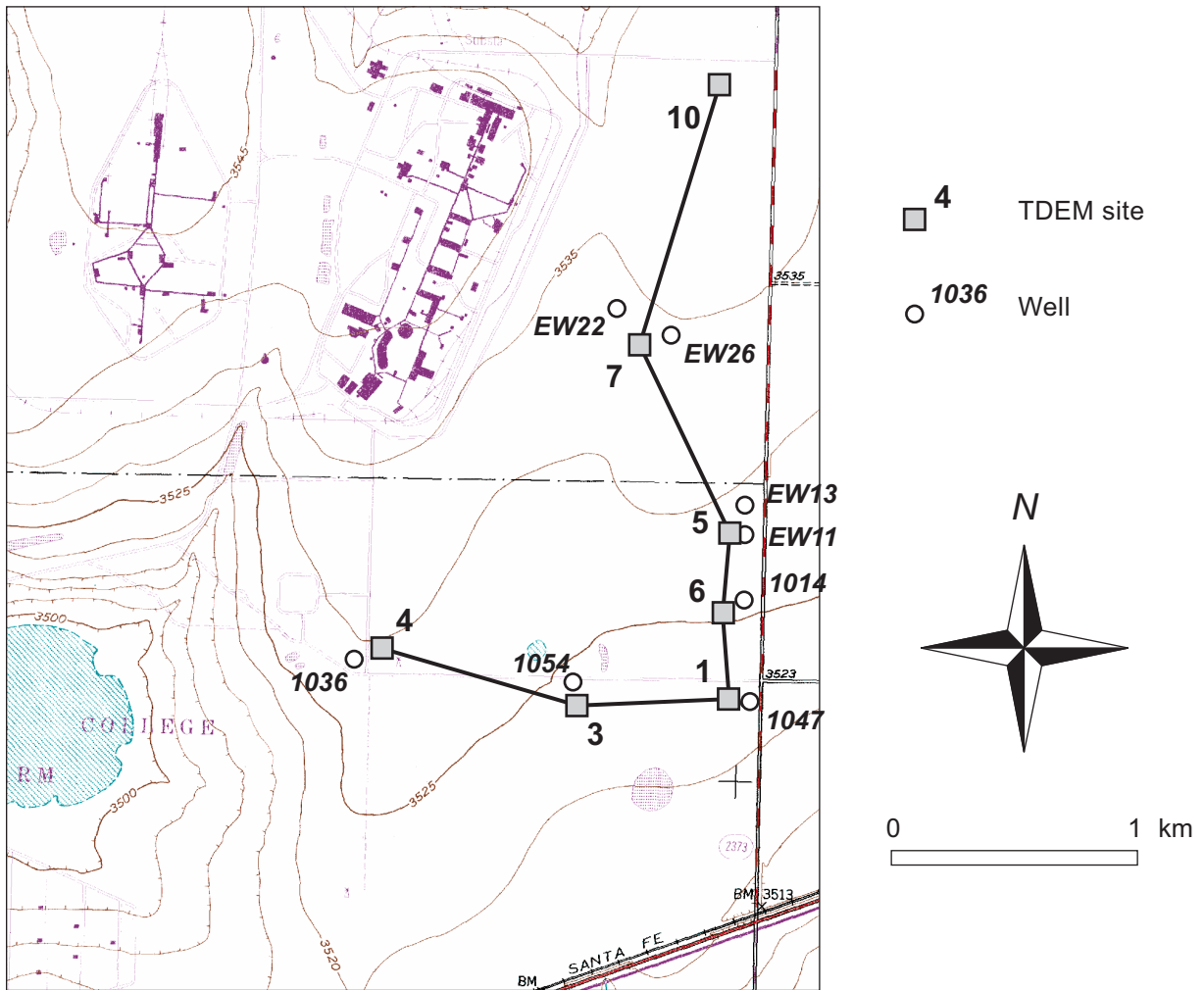


Figure 5. Reconnaissance TDEM sounding sites and nearby water wells in the southeast part of the Pantex Plant.

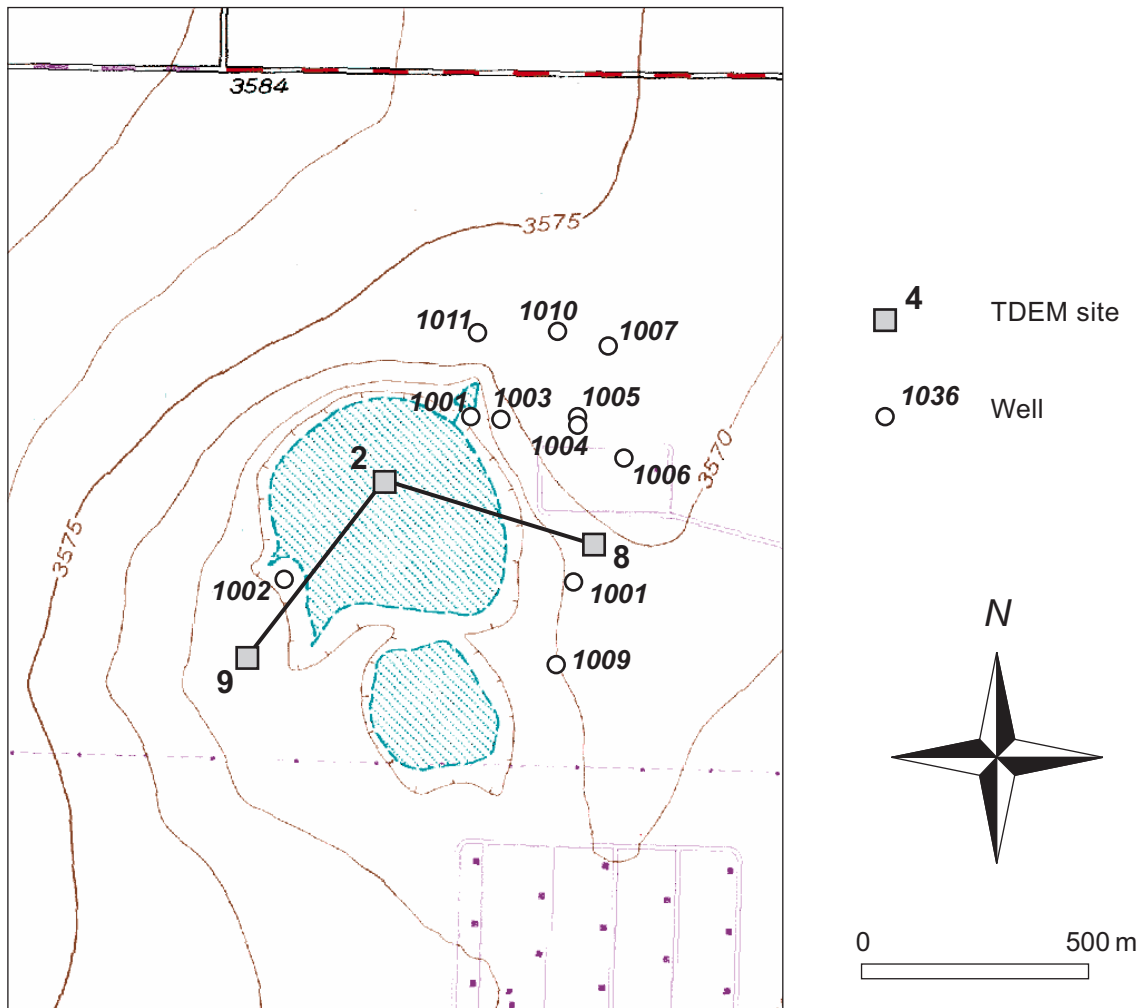


Figure 6. Reconnaissance TDEM sounding sites and nearby water wells in the Playa 3 and Burning Grounds area of the Pantex Plant.

Table 1. Location and elevation of TDEM soundings acquired in the southeast and Playa 3 areas of the Pantex Plant, September 18–22, 2000. Locations are in State Plane Coordinates using the 1927 North American Datum.

**Pantex Southeast soundings** (locations on figure 5)

<b>TDEM site</b>	<b>Northing (ft)</b>	<b>Easting (ft)</b>	<b>Elevation (ft MSL)</b>
1	3752049.632	643704.374	3520.840
3	3751908.566	641601.411	3523.178
4	3752593.997	638980.413	3529.240
5	3754239.125	643696.765	3527.721
6	3753173.721	643530.856	3524.340
7	3756735.732	642301.818	3532.523
10	3760235.112	643288.323	3538.147

**Playa 3 area soundings** (locations on figure 6)

<b>TDEM site</b>	<b>Northing (ft)</b>	<b>Easting (ft)</b>	<b>Elevation (ft MSL)</b>
2	3770291.377	629360.415	3553.776
8	3769907.664	630851.888	3567.891
9	3769021.789	628388.514	3563.159

loop (fig. 7). The area of the transmitter loop was 10,000 m<sup>2</sup>, and the effective area of the receiver coil was 100 m<sup>2</sup>. At typical transmitter current of about 8 amperes, the transmitter dipole moment was 80,000 A-m<sup>2</sup>. We operated the Geonics EM57 transmitter at 30, 7.5, and 3 Hz at each location. Current shutoff times ranged from 38 to 41 microseconds. The resulting transients were measured at 20 time gates ranging from 0.0881 to 6.97 milliseconds (ms) after current shutoff at 30 Hz, 0.352 to 27.9 ms after shutoff at 7.5 Hz, and 0.881 to 70 ms after shutoff at 3 Hz.

TDEM data were processed using TEMIX, a software package published by Interpex. Beginning with one-layer conductivity models, we increased the number of layers at each site until there was no significant decrease in the fitting error (the difference between the observed transient and the transient predicted from the model and the acquisition parameters) when an additional layer was added. Two- to four-layer models generally produced satisfactory fitting errors. Because more than one model can produce a similar transient, we used TEMIX to analyze models that produced equivalent fits to the observed data.

## Modeling Results

The purpose of presurvey TDEM modeling was to determine (a) appropriate acquisition parameters for the field survey and (b) whether anticipated changes in thickness of the FGZ would produce detectable differences in the TDEM data. Very little information has been collected to date on the electrical properties of deposits beneath the Pantex Plant; available data consists of complete induction logs for wells BEG-PTX2 and BEG-PTX3, a few partial induction logs in the Pantex Southeast and Playa 3 areas covering only the well depths below the FGZ, and resistivity logs from public water-supply wells north of the Pantex Plant.

We produced a generalized series of subsurface resistivity models based on resistivity data from well BEG-PTX2, located southwest of Zone 11 and south of Playa 2 (fig. 3). Logs of this and other wells show that resistivity changes within the Blackwater Draw and Ogallala Forma-

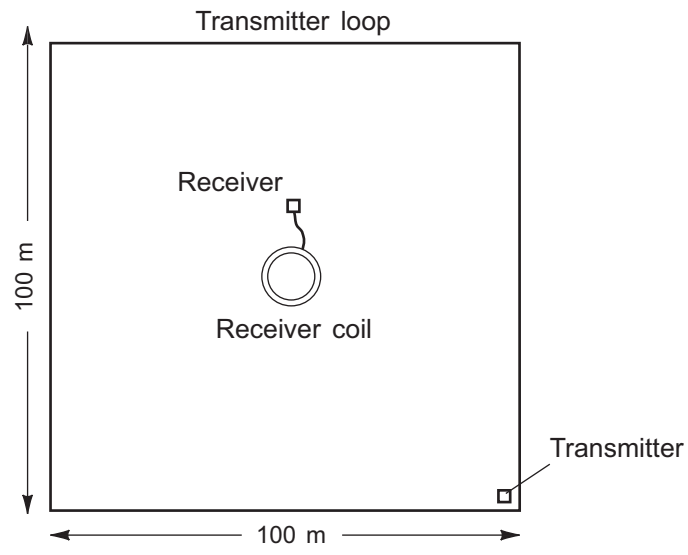


Figure 7. Central loop instrument configuration for TDEM soundings at the Pantex Plant.

tions can be generalized into four layers (fig. 8). These layers are, from shallowest to deepest: (1) a low-resistivity (about 20 ohm-m) layer a few tens of meters thick having high gamma counts and relatively high clay content that roughly corresponds to the Blackwater Draw Formation; (2) an upper Ogallala resistive layer averaging about 75 ohm-m that extends to a depth of about 75 m at BEG-PTX2; (3) a low-resistivity layer of about 9 ohm-m that is about 10-m thick, representing the middle Ogallala FGZ; and (4) a lower Ogallala resistive layer averaging about 45 ohm-m that extends to the base of the Ogallala Formation. Geophysical logs that penetrate pre-Ogallala rocks suggest that the basal Ogallala layer is underlain by a low-resistivity unit, but that unit was not logged in well BEG-PTX2.

To simulate the effect of varying FGZ thicknesses on the TDEM data, we computed and compared the TDEM measurements that would be expected using the resistivities and layer thicknesses of the generalized model, varying the thickness of the FGZ from 0 to 10 m in 1-m increments. Predicted strength of the transient signal differs significantly at times later than about 0.5 ms after shutoff of the transmitter current for the two end-member models of no FGZ and a 10-m-thick FGZ (fig. 9). When the signal strength data are converted to apparent resistivity (fig. 10), the greatest divergence in the curves occurs between about 0.2 and 5 ms after current termination. If the only stratigraphic variable from site to site is the FGZ thickness, modeling data suggest that small changes in FGZ thickness are detectable and that field data should be recorded between about 0.1 and 10 ms after current termination to best detect FGZ thickness changes.

As is clear from the model TDEM data, transient signals decay rapidly to very low levels. To determine whether signal strength would be adequate to overcome EM noise that might be present at the Pantex Plant at sufficiently late times, we used the generalized resistivity model from well BEG-PTX2 to predict signal strength using a range of practical transmitter loop sizes. In general, EM signal strength increases with loop area and loop current. Anticipated noise levels were a few nanovolts per square meter ( $\text{nV}/\text{m}^2$ ). Model results show that transmitter loops smaller than  $80 \times 80$  m would not generate an adequate transient signal at late times, but larger

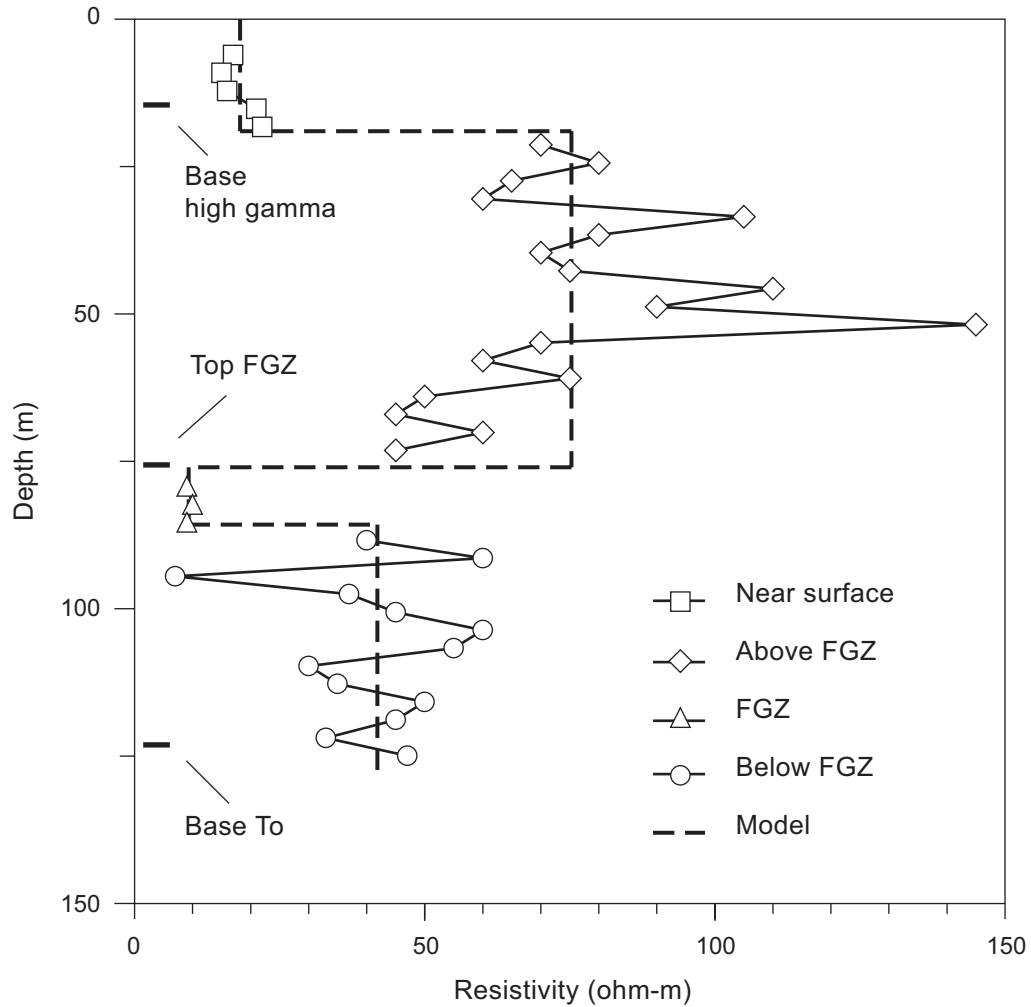


Figure 8. Resistivity log (solid line and symbols) and generalized resistivity model (dashed line) for well BEG-PTX2 in the southwest part of the Pantex Plant. Also shown are the depths at the base of the high-gamma-count zone, the top of the middle Ogallala FGZ, and the base of the Ogallala Formation (To).

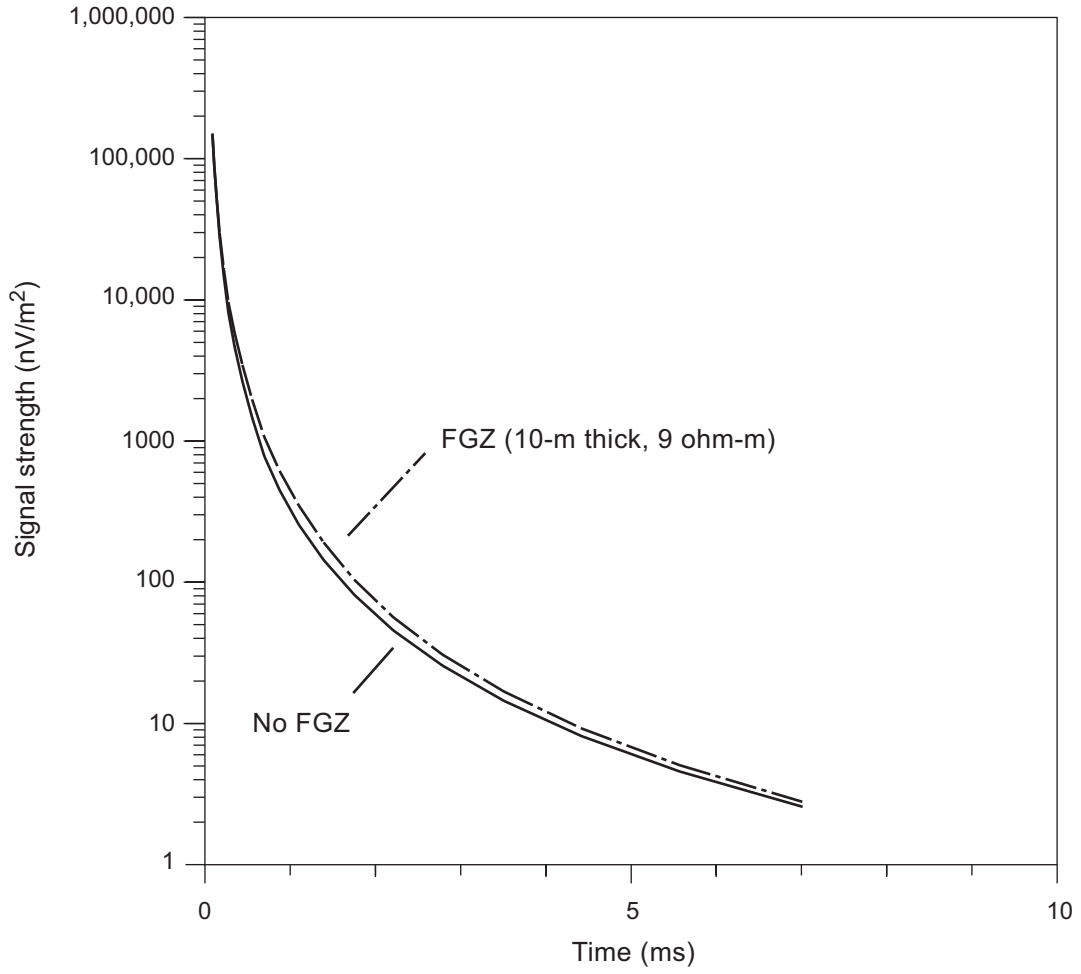


Figure 9. Predicted transient signal for the generalized resistivity model from well BEG-PTX2 with (solid line) and without (dashed line) a 10-m-thick FGZ having 9 ohm-m resistivity.



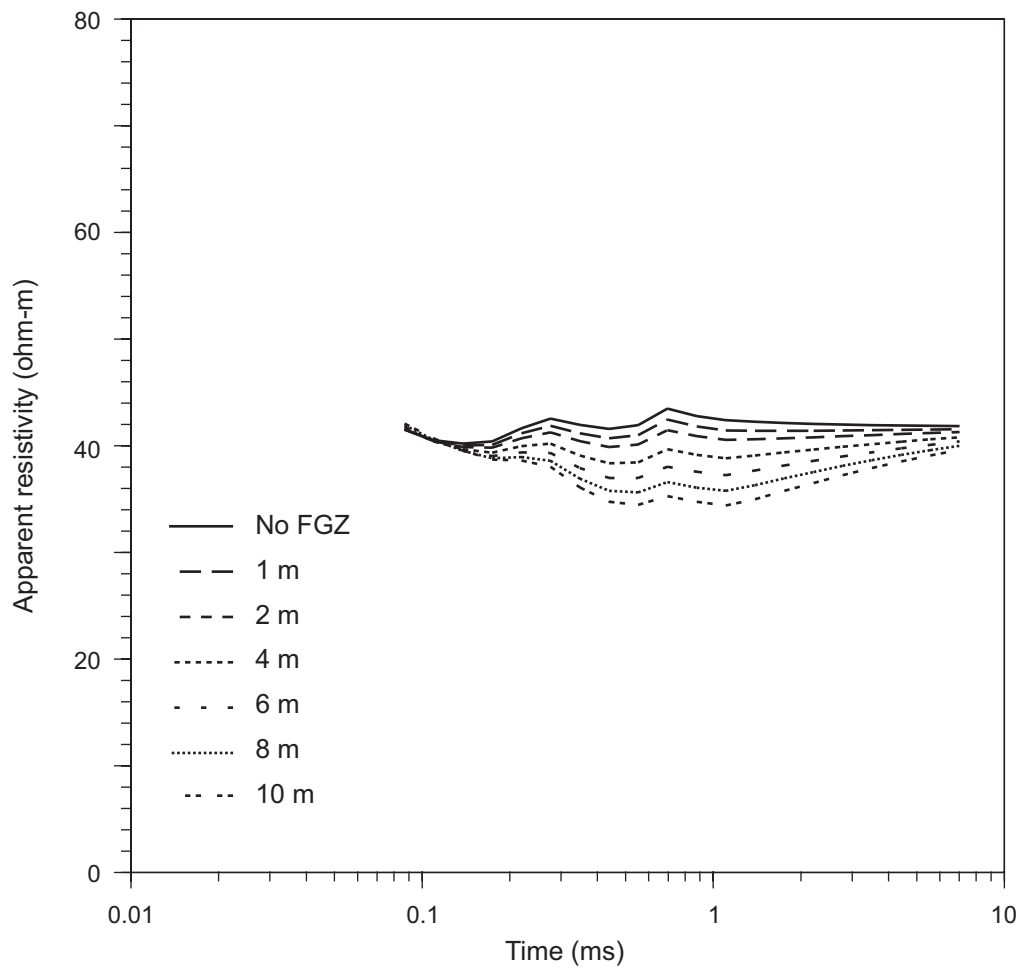


Figure 10. Predicted apparent resistivity curves for the generalized resistivity model from well BEG-PTX2 assuming FGZ thicknesses ranging from 0 (FGZ absent) to 10 m.

loops would (fig. 11). On the basis of these data, we chose to use a  $100 \times 100$ -m transmitter loop in the field study.

We compared results from the BEG-PTX2-based resistivity models with a field-measured transient from site TDEM 4, the sounding acquired closest to the well. Actual data are similar in magnitude to the model data (fig. 12), suggesting that the resistivities used in the model are reasonably close to actual values. Later than about 2 ms after current shutoff, actual signal strength is significantly higher than that computed for the models. The most likely cause of the increased signal strength at late times is the presence of a less resistive unit below the Ogallala that was not logged in well BEG-PTX2.

### Signal Adequacy

Background EM noise is an important potential limitation in TDEM surveys, as is the validity of the assumption of lateral homogeneity of subsurface layers. Once background noise levels and the approximate resistivity of the ground are known in a survey area, transmitter and receiver parameters can be adjusted to provide adequate signal strength to the depth of interest. Because the available TDEM data-processing packages support only the interpretation of  $z$ -axis (vertical dipole) data, it is important that there be no large lateral changes in resistivity at depth near the TDEM sounding. Lateral changes in layer resistivity produce a horizontal (three-dimensional) component in the transient, which can affect the  $z$ -axis measurements and the resulting models that are constructed to fit the observed transient. Until true three-dimensional processing algorithms are developed, we evaluate the validity of the lateral homogeneity assumption at the survey scale by acquiring  $x$ - and  $y$ -axis (horizontal dipole) data and comparing those signals with  $z$ -axis signals.

We measured background noise at each TDEM site by shutting off the transmitter while recording data with the receiver in position to collect  $z$ -axis data. In general, noise levels were relatively low at each of the 10 field sites. Noise levels were somewhat higher in the Pantex

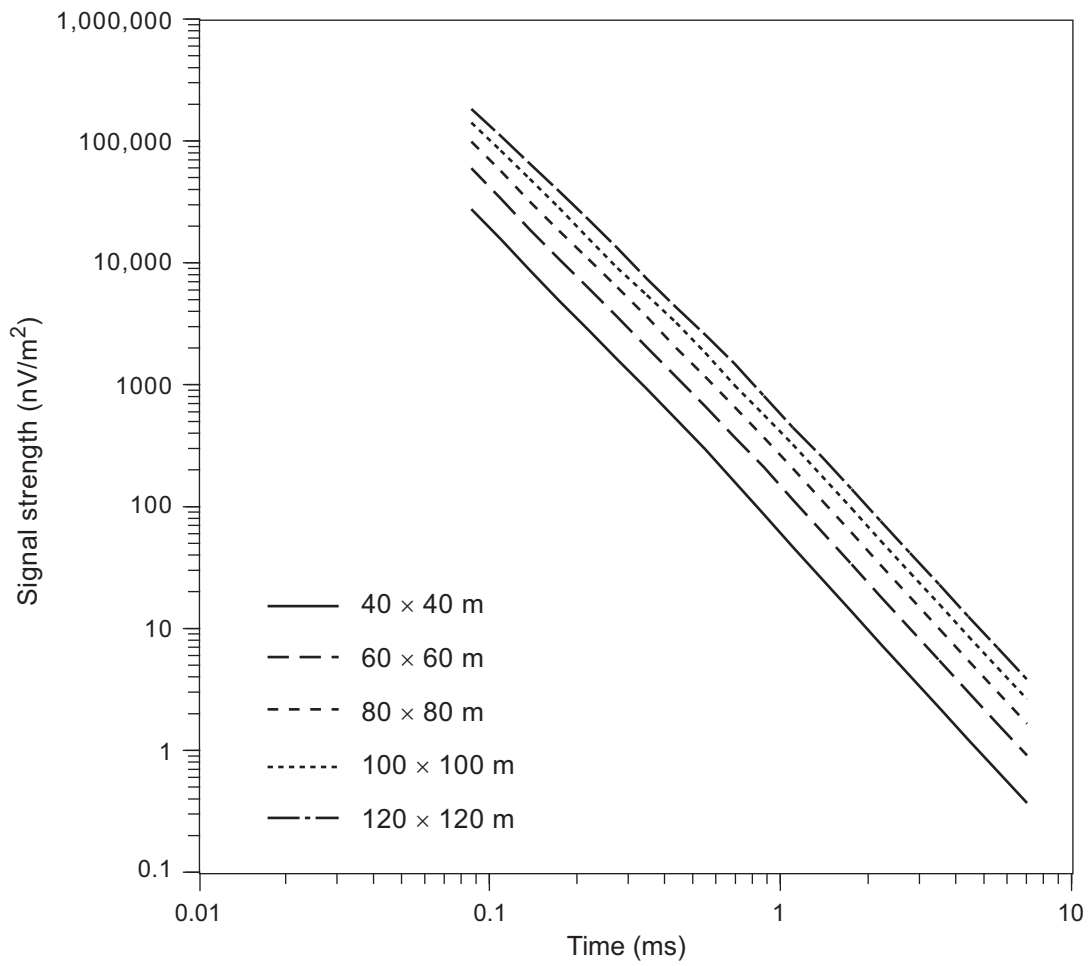


Figure 11. Predicted transient signal for the generalized resistivity model from well BEG-PTX2 assuming a transmitter loop current of 18 amperes and loop sizes ranging from 40 × 40 m to 120 × 120 m.

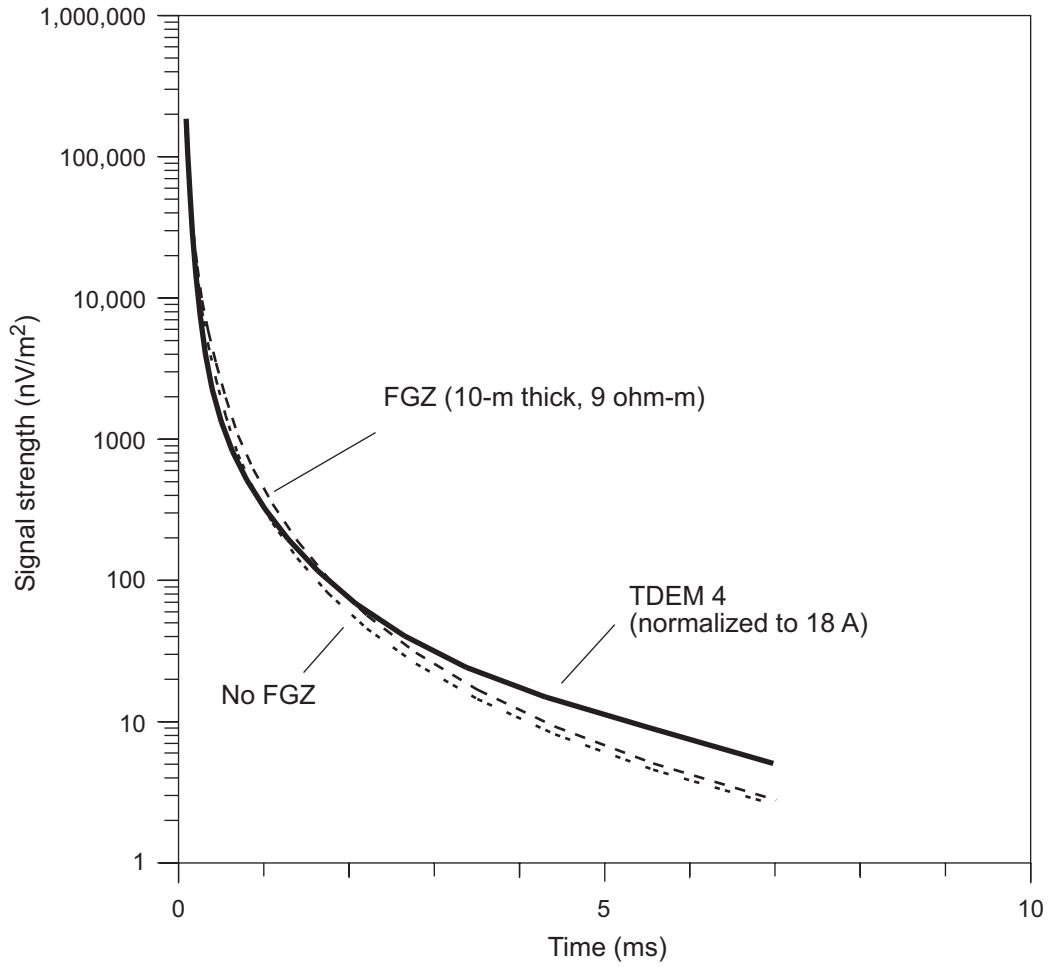


Figure 12. Comparison of actual transient recorded at site TDEM 4 with the transients predicted for the generalized resistivity models (FGZ and no FGZ) from well BEG-PTX2.

Southeast area than they were in the Playa 3 area. A comparison of signal strength with the transmitter on and off at TDEM 7 in the Pantex Southeast area showed signals exceeding noise at times as late as 7 ms after current shutoff (fig. 13). Noise levels in this area are typically between about 0.1 and 1 nV/m<sup>2</sup>. At sounding TDEM 8 near Playa 3, signal strength is similar to that in the Pantex Southeast area, but noise levels are considerably lower (fig. 14). Noise levels vary through time and from site to site owing to a variety of factors that include electrical storm activity and proximity to power lines and electric motors. Noise levels are monitored in the field during an EM survey.

We tested the lateral homogeneity assumption by acquiring *x*-, *y*-, and *z*-axis data at each site while the transmitter was operating. Ideally, the *z*-axis signal would be the strongest signal at all measured times, and the much weaker horizontal components would approximately equal each other. During our reconnaissance survey, data from most sites showed that *z*-axis signals were one or more orders of magnitude stronger than *x*- and *y*-axis signals and that *x*- and *y*-axis signals were approximately equal (such as was observed at site TDEM 9 near Playa 3, fig. 15), thus validating the homogeneity assumption at each sounding site. Only data recorded at site TDEM 4 in the Pantex Southeast area show a relatively strong horizontal component, particularly for the *x*-axis data oriented east–west (fig. 16). These data suggest that the lateral homogeneity assumption is invalid at the sounding scale at site TDEM 4 and that models derived from the *z*-axis data at that site may be in error, particularly at later times and deeper model depths.

### Pantex Southeast Results

We acquired seven TDEM soundings in the Pantex Southeast area (fig. 5), all but one of which were near existing wells. These soundings can be examined as a series oriented approximately west–east (sites TDEM 4, 3, and 1) and a series oriented approximately south–north (sites TDEM 1, 6, 5, 7, and 10). No borehole conductivity data exist over the appropriate depth range to compare surface and borehole measurements.

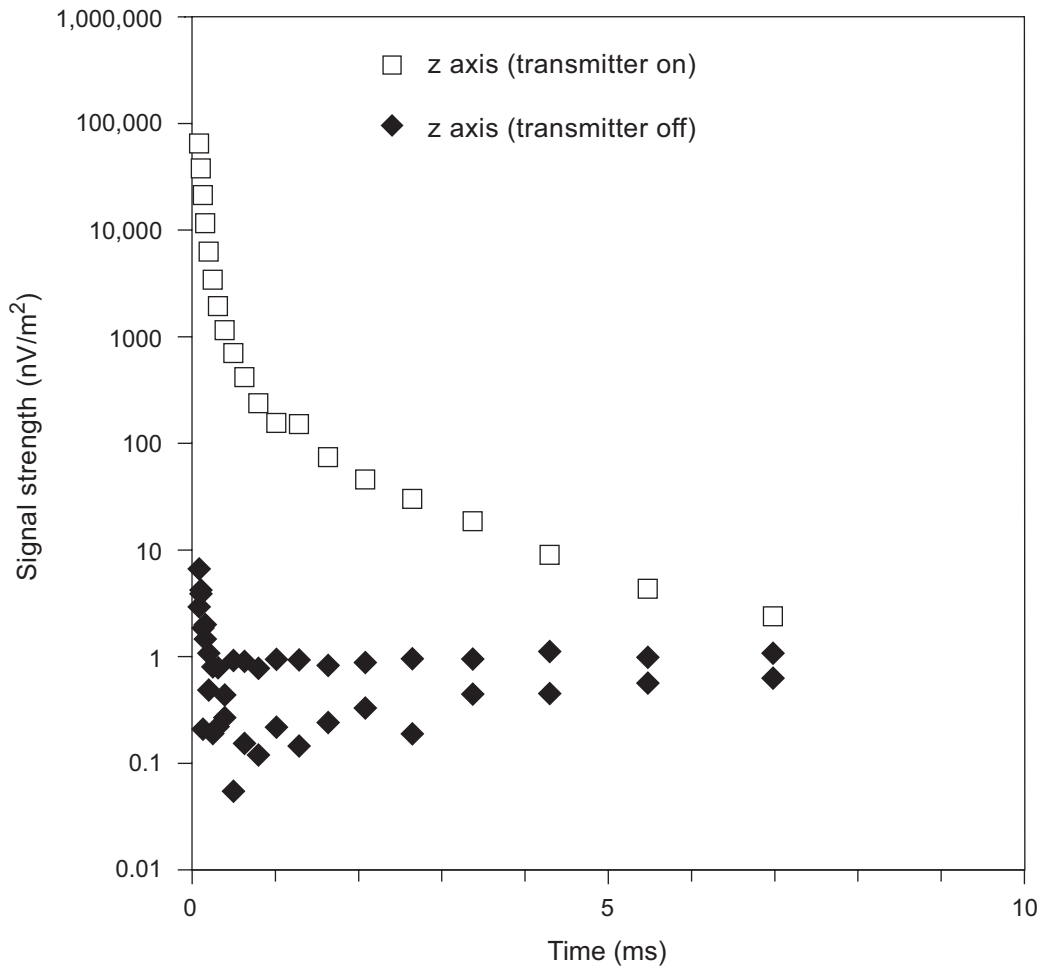


Figure 13. Comparison of transient signal (open squares) with background noise (solid diamonds) for z-axis data at site TDEM 7 in the Pantex Southeast area.

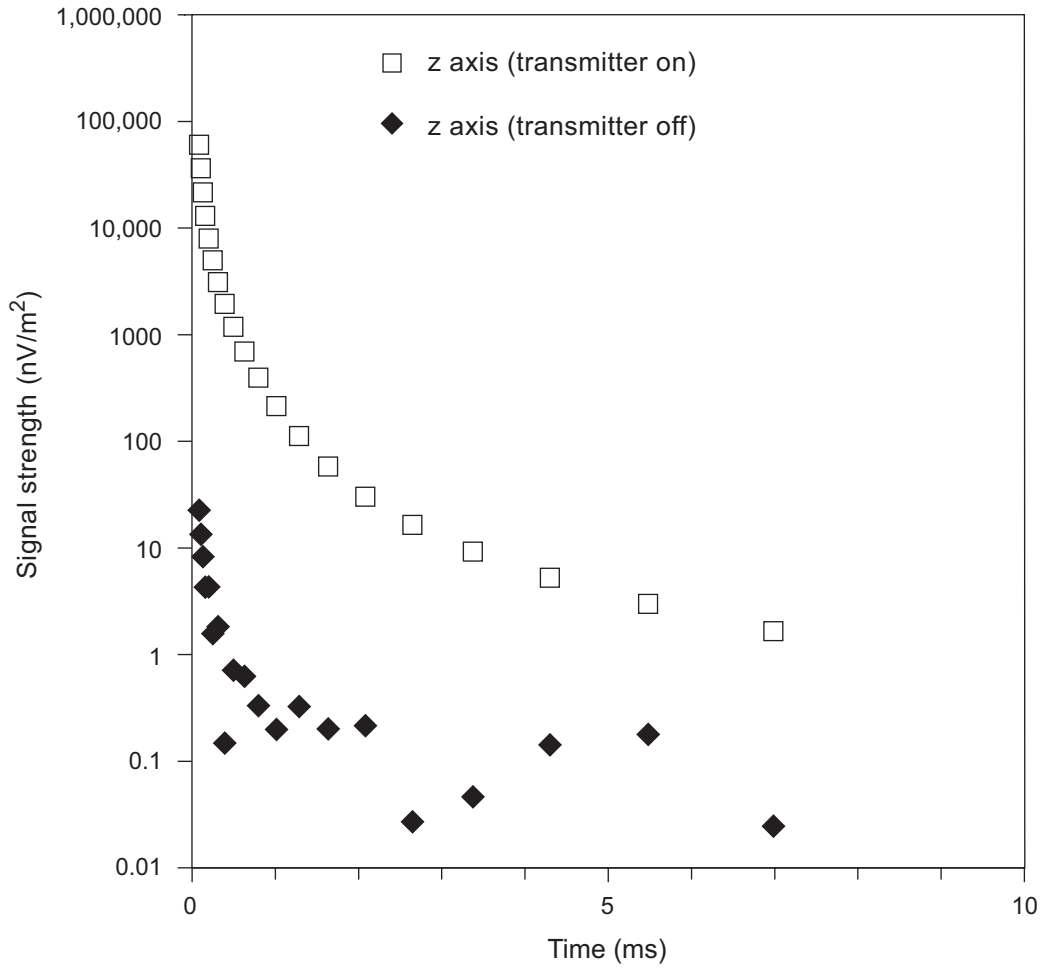


Figure 14. Comparison of transient signal (open squares) with background noise (solid diamonds) for z-axis data at site TDEM 8 in the Playa 3 area.

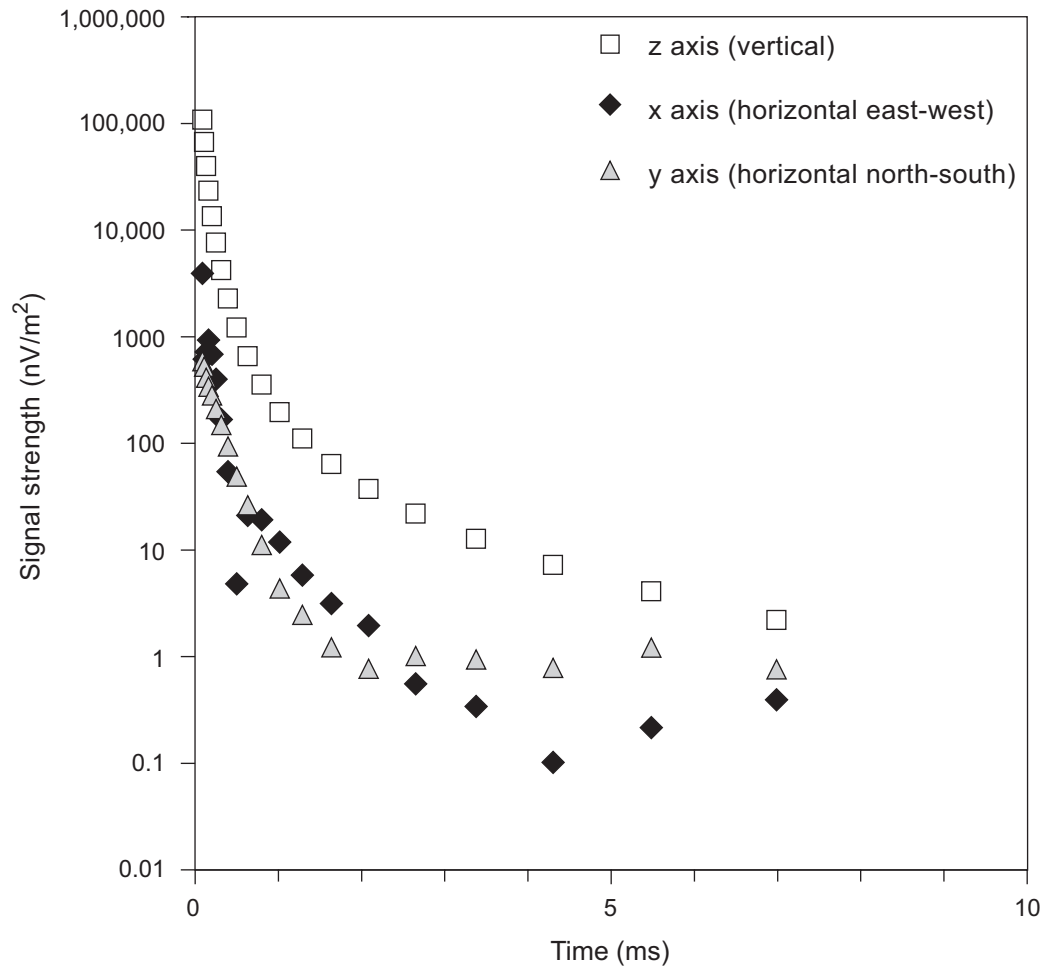


Figure 15. Comparison of z-axis (vertical component) transient (open squares) with x- and y-axis (horizontal component) transients (solid and shaded symbols) recorded with the transmitter operating at site TDEM 9 in the Playa 3 area.



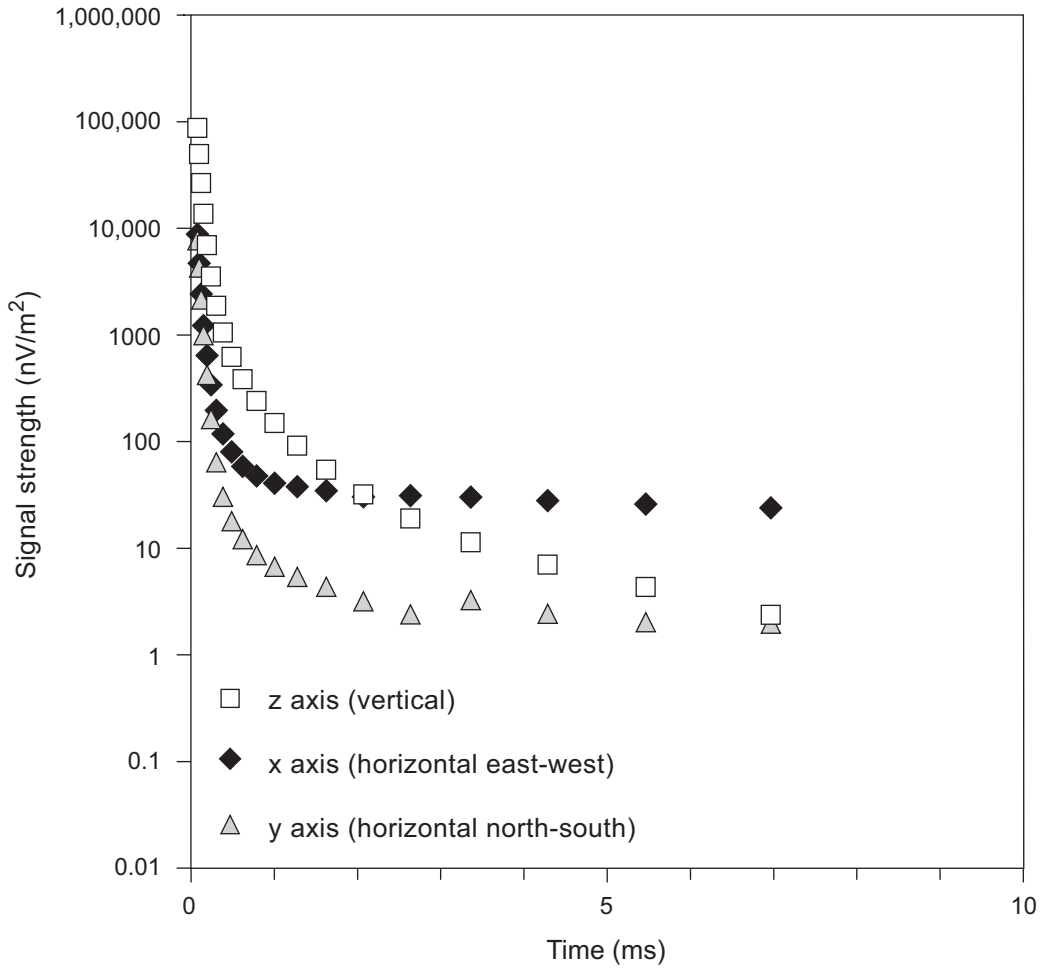


Figure 16. Comparison of *z*-axis (vertical component) transient (open squares) with *x*- and *y*-axis (horizontal component) transients (solid and shaded symbols) recorded with the transmitter operating at site TDEM 4 in the Pantex Southeast area.

Transient signals recorded along the west–east series (fig. 17) and the south–north series (fig. 18) show similar trends. At early times of 0.1 ms or less after transmitter current shutoff, signal strengths approach 100,000 nV/m<sup>2</sup>. Depending on location, these strong early signals decay at differing rates to a few nV/m<sup>2</sup> at the latest times displayed. According to modeling results, these signals are sufficiently long to contain information about subsurface electrical properties to depths beyond those of the FGZ. Changes in slope of each decay curve result from changes in electrical properties encountered as the primary signal travels deeper into the subsurface. Variability among transients within both the west–east and south–north series indicates that the subsurface resistivity profile differs from site to site.

General subsurface changes in resistivity with depth can be inferred by recasting the signal strength curves into changes in apparent resistivity with time. Every apparent resistivity curve for both the west–east (fig. 19) and south–north (fig. 20) series indicates relatively low apparent resistivity at the earliest times, highest apparent resistivity at times between 0.1 and 1 ms, and decreasing apparent resistivity at later times. In a simplified sense, the shapes of the apparent resistivity curves suggest that the Pantex Southeast area is underlain by a surface layer of low resistivity, a resistive underlying layer, and a low-resistivity basal layer. This configuration matches the gross shape of the generalized resistivity log at well BEG-PTX2. The curves also show that the bulk resistivity of the Pantex Southeast area is in the 20- to 60-ohm-m range.

Differences in the apparent resistivity curves for individual soundings further suggest that the TDEM soundings are detecting lateral changes in subsurface electrical properties. At sounding TDEM 1, for example, higher resistivities at early times suggest a more resistive surface layer than at the other two sites on the west–east series (fig. 19). Higher apparent resistivities at later times for soundings TDEM 3 and 4 suggest that, at some deeper depth, the material beneath those sites is more resistive than that beneath sounding TDEM 1. Similarly, the most resistive near-surface layer (or the thinnest overlying conductive layer) most likely lies beneath site TDEM 6 on the south–north series (fig. 20), whereas the most resistive deeper layers should be encountered beneath site TDEM 10 near the Pantex East gate.

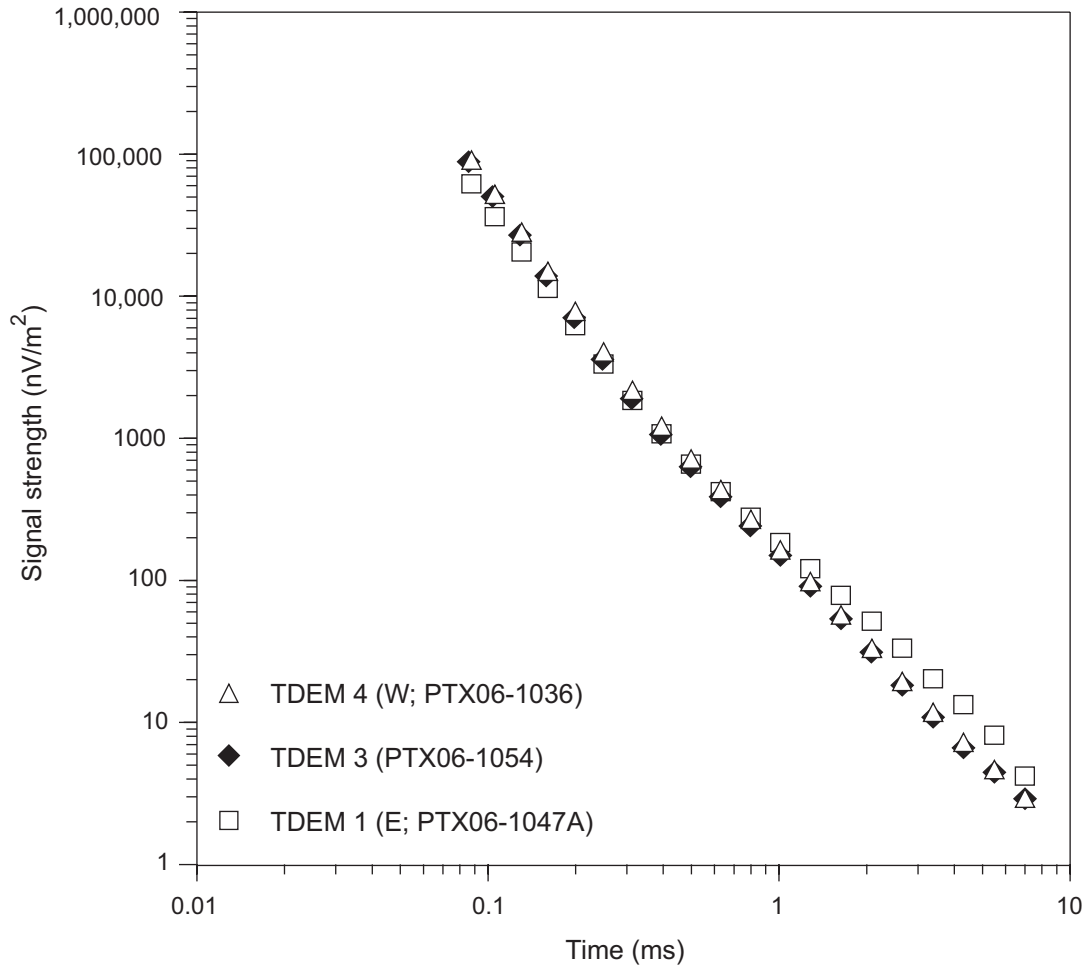


Figure 17. Transients recorded at sites TDEM 4, 3, and 1 along a west–east series in the Pantex Southeast area (fig. 5). Also listed are adjacent wells.

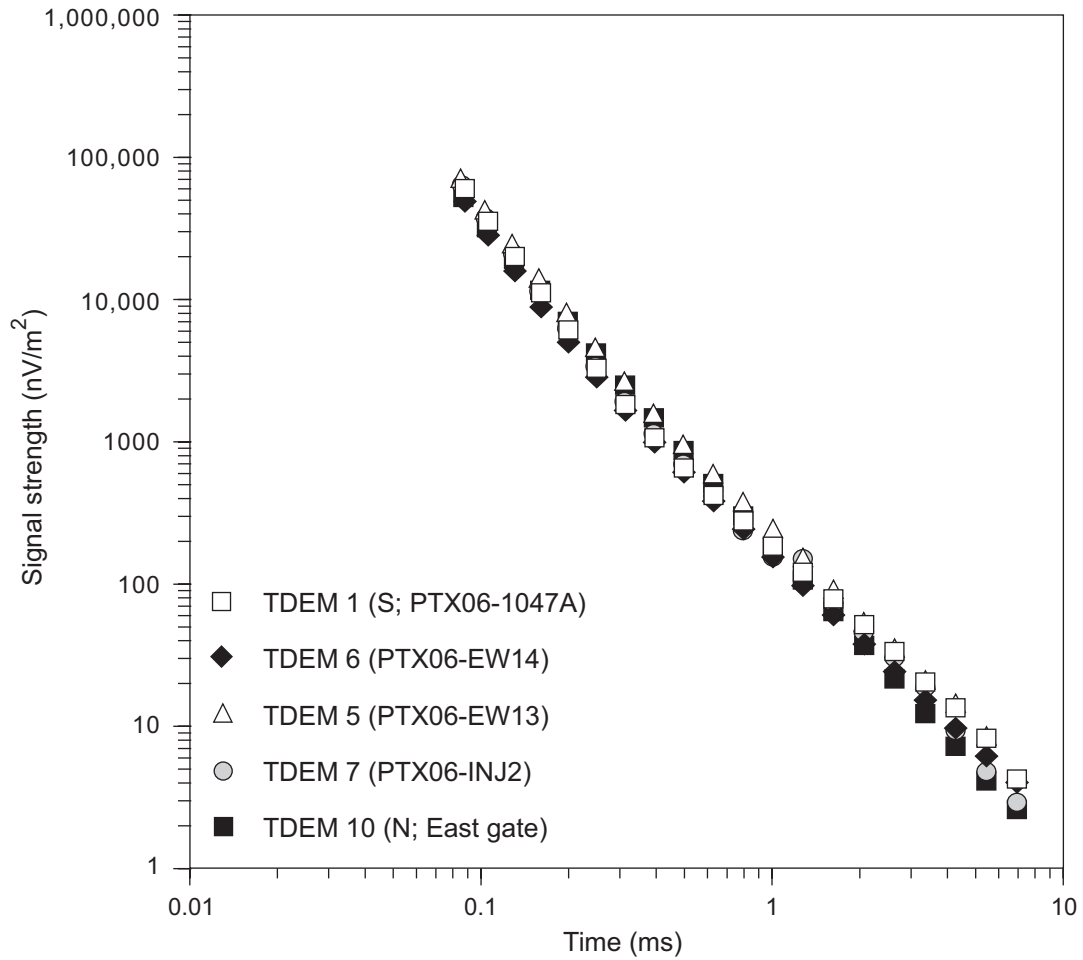


Figure 18. Transients recorded at sites TDEM 1, 6, 5, 7, and 10 along a south–north series in the Pantex Southeast area (fig. 5). Also listed are adjacent wells or landmarks.

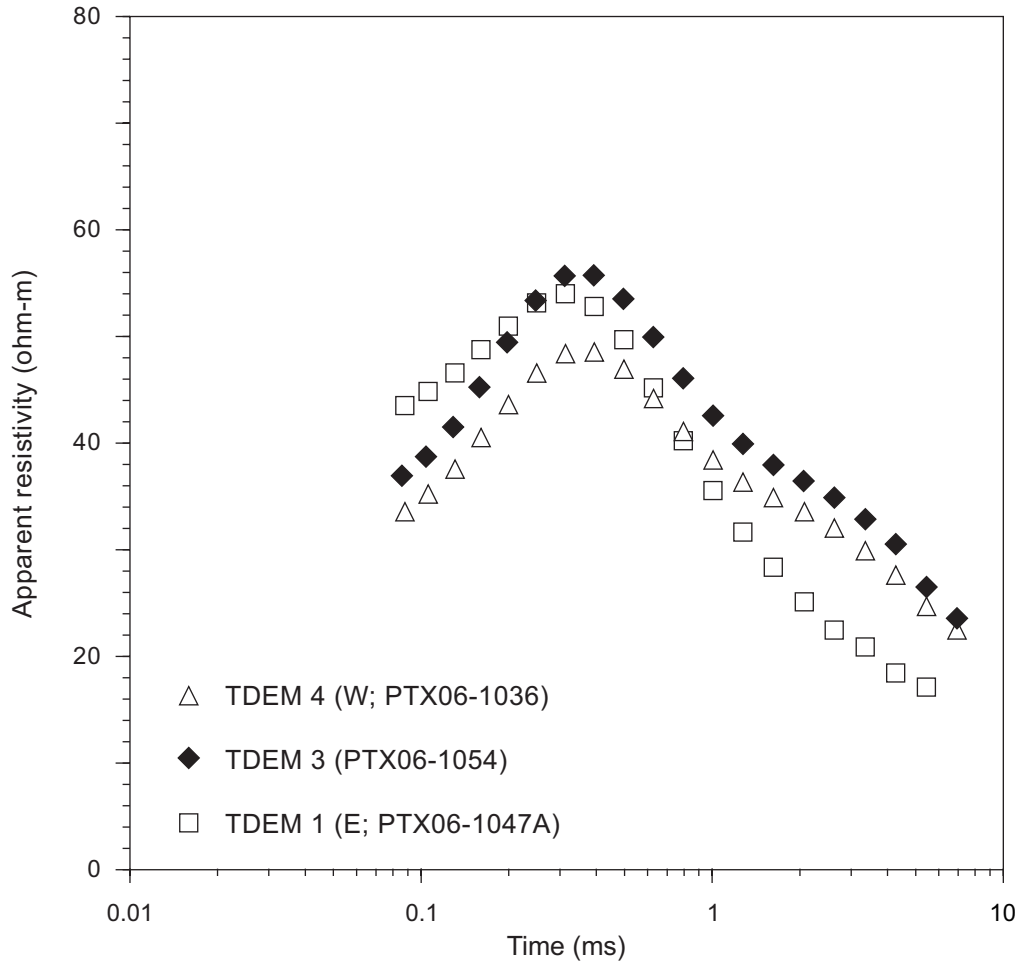


Figure 19. Apparent resistivity curves calculated for transients recorded at sites TDEM 4, 3, and 1 along a west–east series in the Pantex Southeast area (fig. 5). Also listed are adjacent wells.

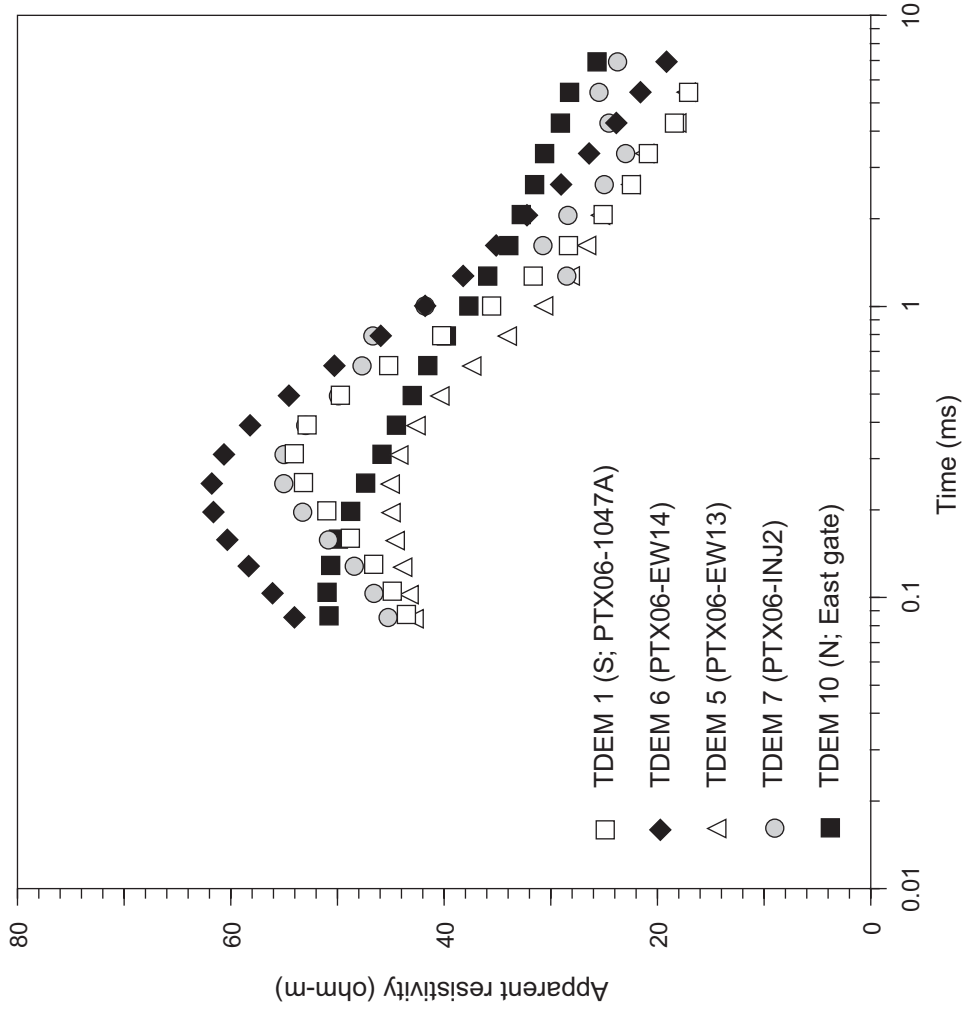


Figure 20. Apparent resistivity curves calculated for transients recorded at sites TDEM 1, 6, 5, 7, and 10 along a south–north series in the Pantex Southeast area. Also listed are adjacent wells or landmarks.

Using the TEMIX data-processing and analysis software, we constructed resistivity models of the subsurface, calculated the transient for those models, compared the calculated transients with the actual transient, and adjusted the model iteratively until it provided an adequate fit to the observed data. Using data from sounding TDEM 1 as an example (fig. 21), the best fit we could obtain with a one-layer model resulted in a synthetic transient that differed from the actual transient by 73 percent. Adding a second layer reduced the fitting error to less than 8 percent. Adding a third layer and adjusting layer thicknesses and resistivities produced a fitting error of less than 4 percent, which did not improve significantly with the addition of more layers. The synthetic transient calculated for the three-layer model closely approximated the actual transient at that site. As was suggested by the apparent resistivity curves, the best-fit model consisted of a low-resistivity surface layer, a high-resistivity intermediate layer, and a low-resistivity basal layer. Although an FGZ could be added to the model at the appropriate depth and a good fit obtained, one is not necessary to adequately fit the observed data.

Best-fit models constructed similarly for the other soundings in the Pantex Southeast area (table 2) show similar resistivity trends with depth. On the west–east series, the low-resistivity surface layer at TDEM 3 and 4 approximately correlates with the high-gamma-count zone detected in borehole logs (fig. 22). The FGZ, detected at a depth of about 80 m in nearby wells, is not resolved in the models. The sharp decrease in resistivity modeled deeper than 100 m occurs near the Ogallala water level and near the base of the Ogallala. Lowest resistivities at the FGZ level are at TDEM 3, suggesting higher clay content or a thicker FGZ at this site than at the other two sites on the west–east series.

Two- to four-layer models constructed for soundings along the south–north series differ relatively little in the near-surface low-resistivity layer (fig. 23) but differ more at deeper levels. Within what would correspond to the upper Ogallala resistive zone and the middle Ogallala FGZ, resistivities decrease progressively to the north. Highest resistivities at the FGZ depth are calculated for sounding TDEM 1 at the south end of the series; lowest resistivities are calculated for TDEM 10 near the Pantex East gate. Maps of the FGZ thickness derived from Ebasco seismic

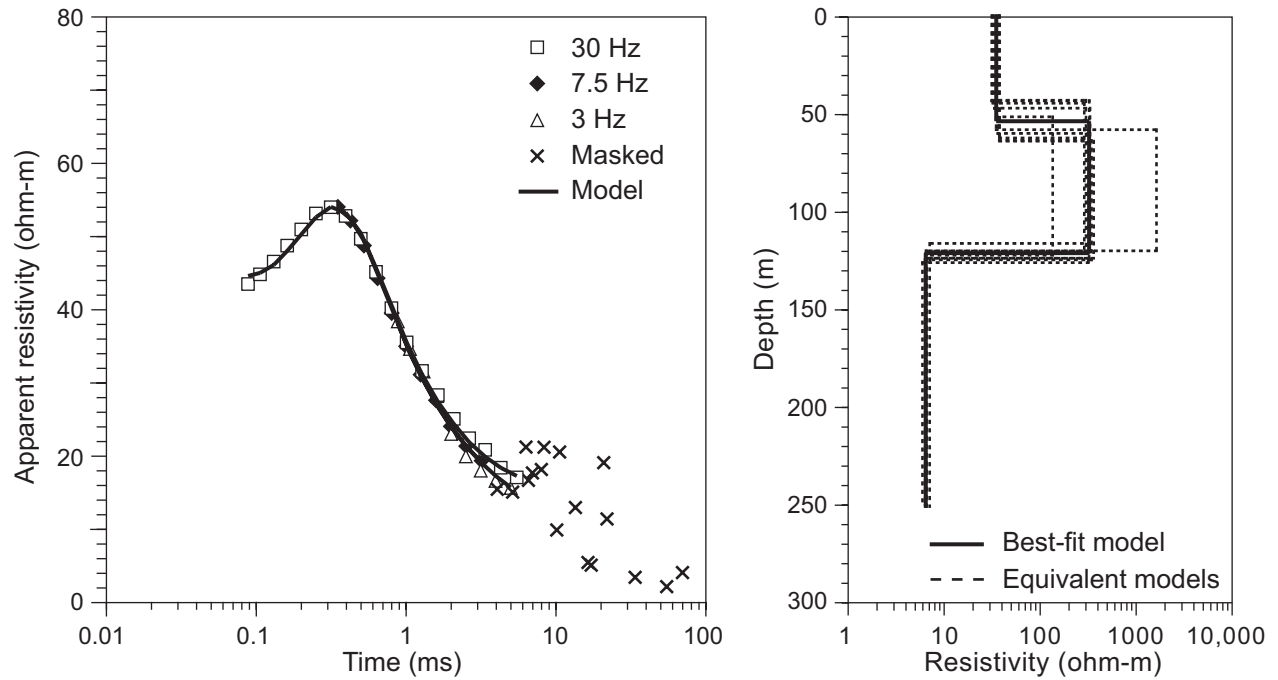


Figure 21. (left) Apparent resistivity data recorded at site TDEM 1 with the transmitter operating at 30, 7.5, and 3 Hz (squares, diamonds, and triangles); masked data; and the synthetic apparent resistivity curves (solid lines) calculated from the (right) best-fit and equivalent-fit resistivity models.



Table 2. Best-fit models for TDEM soundings in the Pantex Southeast area. Locations on figure 5.

Layer	Resistivity (ohm-m)	Thickness (m)	Conductivity (mS/m)	Depth to top (m)	Depth to base (m)	Elevation at top (m MSL)	Elevation at base (m MSL)
TDEM 1 (Fitting error 3.8 %)							
1	34.9	53.7	28.7	0.0	53.7	1073.2	1019.4
2	324.4	67.3	3.1	53.7	121.0	1019.4	952.2
3	6.4		155.5	121.0		952.2	
TDEM 3 (Fitting error 7.1 %)							
1	21.5	26.7	46.6	0.0	26.7	1073.2	1046.5
2	190.6	84.7	5.2	26.7	111.4	1046.5	961.8
3	15.6		64.0	111.4		961.8	
TDEM 4 (Fitting error 7.9 %)							
1	18.3	19.1	54.6	0.0	19.1	1075.7	1056.6
2	208.1	97.0	4.8	19.1	116.1	1056.6	959.7
3	14.8		67.5	116.1		959.7	
TDEM 5 (Fitting error 3.9 %)							
1	32.3	46.6	30.9	0.0	46.6	1075.2	1028.5
2	110.4	51.5	9.1	46.6	98.1	1028.5	977.0
3	10.7	93.7	93.2	98.1	191.8	977.0	883.3
4	6.2		161.6	191.8		883.3	
TDEM 6 (Fitting error 3.2 %)							
1	40.0	43.8	25.0	0.0	43.8	1074.2	1030.4
2	165.5	68.9	6.0	43.8	112.7	1030.4	961.6
3	12.6	103.3	79.7	112.7	216.0	961.6	858.3
4	5.3		189.0	216.0		858.3	
TDEM 7 (Fitting error 12.1 %)							
1	34.1	35.1	29.3	0.0	35.1	1076.7	1041.7
2	76.2	100.4	13.1	35.1	135.5	1041.7	941.3
3	8.7	90.6	115.3	135.5	226.1	941.3	850.6
4	44.8		22.3	226.1		850.6	
TDEM 10 (Fitting error 4.0 %)							
1	42.4	125.3	23.6	0.0	125.3	1078.4	953.1
2	18.4		54.3	125.3		953.1	

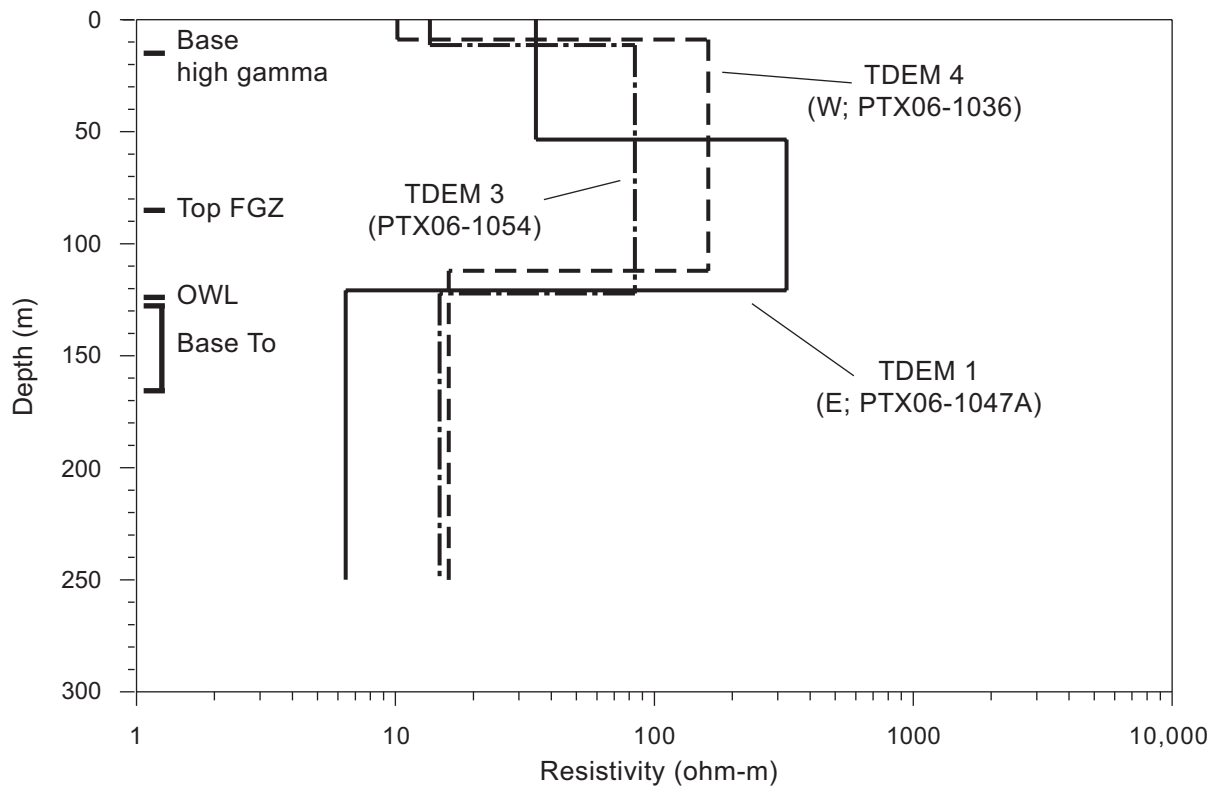


Figure 22. Three-layer resistivity models that fit transients recorded at sites TDEM 4, 3, and 1 in the Pantex Southeast area. Also shown are the approximate depths to the base of the high-gamma-count zone, the top of the middle Ogallala FGZ, the Ogallala water level (OWL), and the base of the Ogallala Formation (To).

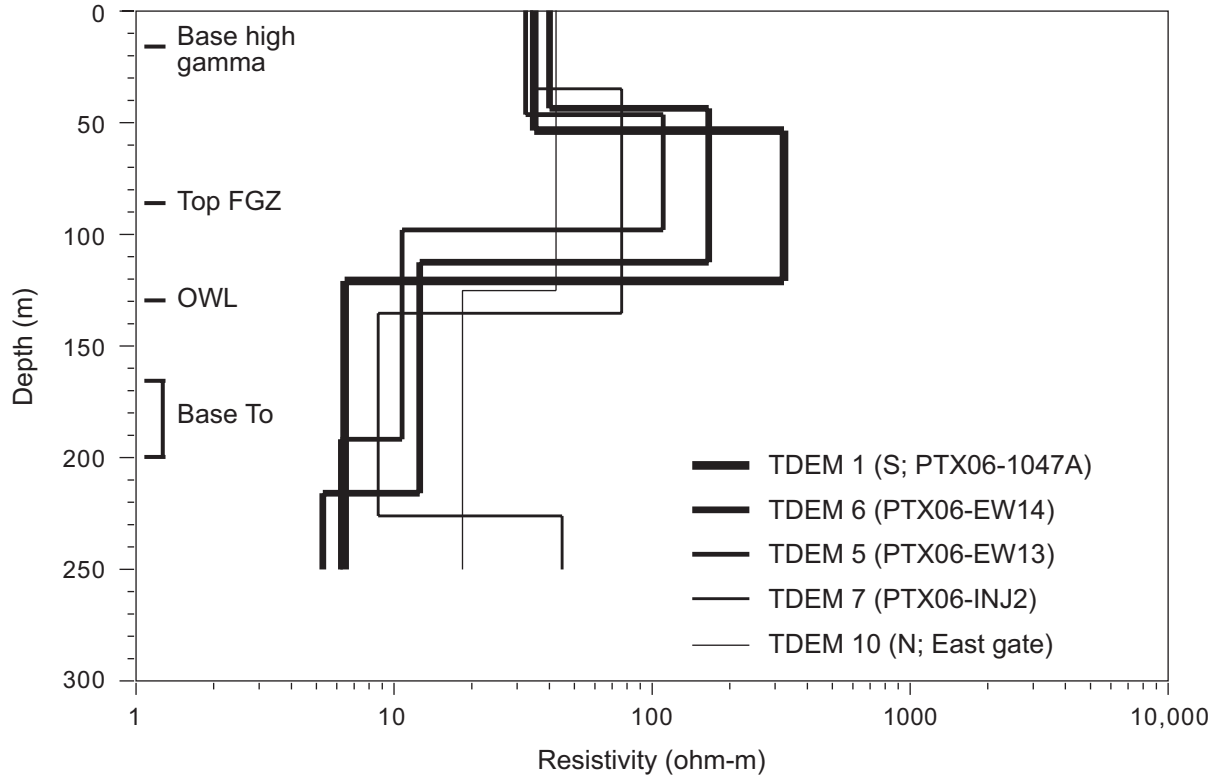


Figure 23. Two- to four-layer resistivity models that fit transients recorded at sites TDEM 1, 6, 5, 7, and 10 in the Pantex Southeast area. Also shown are the approximate depths to the base of the high-gamma-count zone, the top of the middle Ogallala FGZ, the Ogallala water level (OWL), and the base of the Ogallala Formation (To).

data (U.S. Army Corps of Engineers, 1992) show the FGZ thickness progressively increasing northward along this series, matching the TDEM trend. Again, the FGZ does not appear in the model as a discrete, resolvable layer, but apparently it is a major influence on resistivity calculated for the resistive intermediate layer. Decreases in resistivity to near 10 ohm-m in the model layers corresponding to the lower part of the Ogallala occur near the depth reported for the Ogallala water level. Further resistivity changes at deeper depths in the models are at or deeper than the reported base of the Ogallala.

### Playa 3 Area Results

We acquired three TDEM soundings in the Playa 3 and Burning Grounds area (fig. 6). One sounding, TDEM 2, was located on the dry floor of the playa; the other two were located on the flanks of the basin surrounding the playa. Transient signal strength was similar to that recorded in the Pantex Southeast area for the soundings TDEM 8 and 9 on the flank of the basin, decreasing from near 100,000 nV/m<sup>2</sup> at the earliest times recorded to less than 2 nV/m<sup>2</sup> at late times (fig. 24). The playa floor sounding produced a similar late-time transient but exhibited significantly higher signal strength at times earlier than 1 ms.

Soundings TDEM 8 and 9 on the flanks of the playa basin have apparent resistivities in the same 20 to 60 ohm-m range as was observed in the Pantex Southeast area but differ in shape (fig. 25). Lowest apparent resistivities at early times (shallow depths) are calculated for sounding TDEM 2 on the playa floor. Intermediate apparent resistivities are recorded at early times for sounding TDEM 9, which is situated well within the playa basin at an elevation only about 3 m higher than that of the playa floor sounding (table 1). Highest apparent resistivities at early times were recorded at sounding TDEM 8, the sounding nearest the edge of the topographic basin surrounding Playa 3.

At each Playa 3 sounding, best-fit resistivity models constructed for the observed transients include a near-surface layer of relatively low resistivity underlain by a more resistive layer

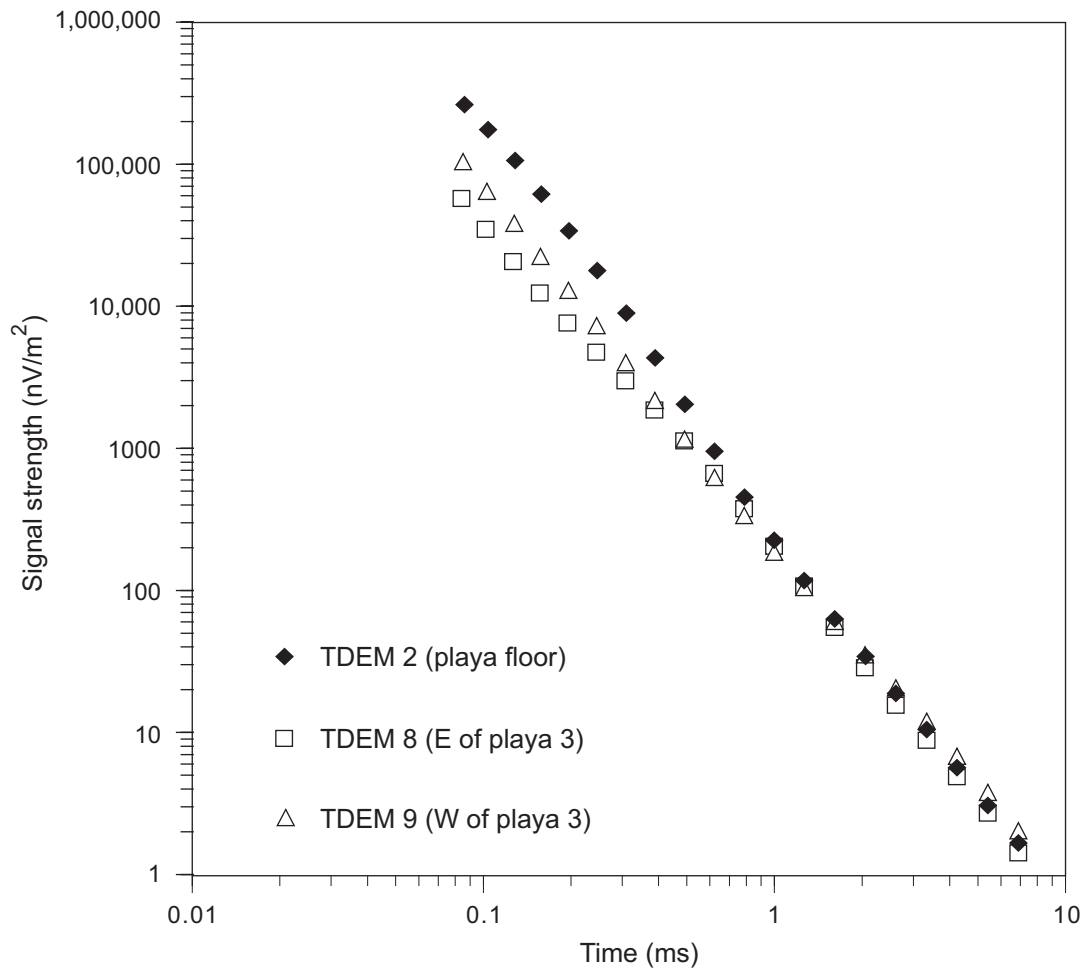


Figure 24. Transients recorded at sites TDEM 2, 8, and 9 in the Playa 3 area (fig. 6).

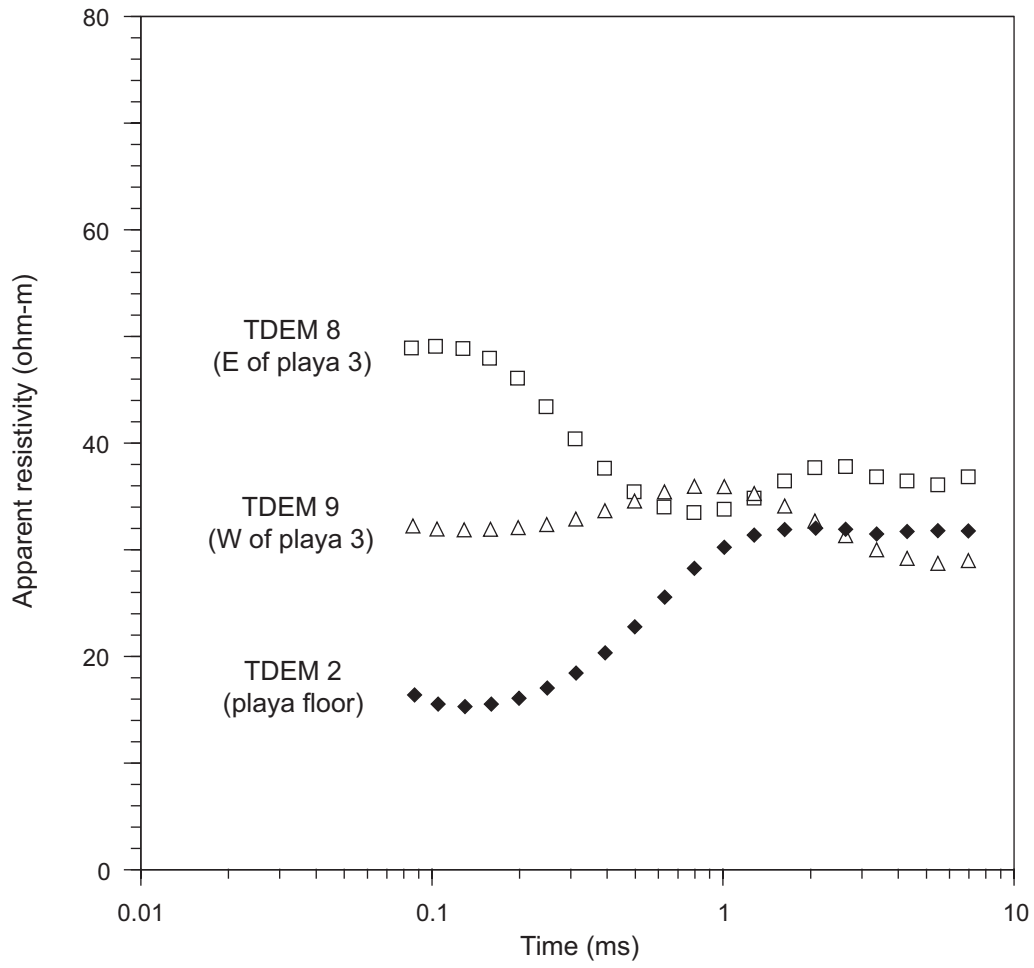


Figure 25. Apparent resistivity curves calculated for transients recorded at sites TDEM 2, 8, and 9 in the Playa 3 area.

(fig. 26; table 3). The best-fit model for sounding TDEM 8, located on the flank of the basin south of the Burning Grounds, is the only one that requires a thin, low-resistivity layer near the depth reported for the FGZ in nearby wells. At TDEM 9, southwest of the playa, the top of a low-resistivity layer is modeled near the reported Ogallala water level. The best-fit model constructed for TDEM 2, the playa floor sounding, has both the lowest resistivity surface layer and the highest resistivity intermediate layer. The low-resistivity layer at the surface can be interpreted as a clay-rich unit that is a few tens of meters thick. The highly resistive layer just below this might represent either relatively coarse deposits beneath the surface clayey layer or disturbed deposits with abundant void space. When these observations are combined with observations made from seismic reflection data acquired across Playa 3, both data types suggest that strata beneath the playa differ significantly from strata outside the playa basin.

#### SEISMIC REFLECTION SUMMARY AND RECOMMENDATIONS

The seismic reflection surveys conducted in the early 1990's by Ebasco for the U.S. Army Corps of Engineers and those conducted by the Bureau both had broad depth objectives that ranged from the Ogallala caprock at depths of 30 m or less to the base of the Ogallala Formation at depths greater than 200 m. Both surveys provided basic data on the stratigraphic framework of playa and interplaya areas. Data acquisition parameters and processing procedures for those surveys were selected on the basis of those relatively broad depth objectives, which might not enhance reflections associated with the FGZ. Although the top of the FGZ appears to be a good seismic reflector in existing data, reprocessing the limited Ebasco and Bureau seismic data in the Pantex Southeast area might enhance that reflection and reveal other associated reflectors in the same intermediate depth range.

Reprocessing existing seismic data might provide incremental improvement in detecting the presence and resolving the thickness of the FGZ. Further improvement in the seismic characterization of the FGZ would require acquisition of new seismic data in priority areas such as Pantex

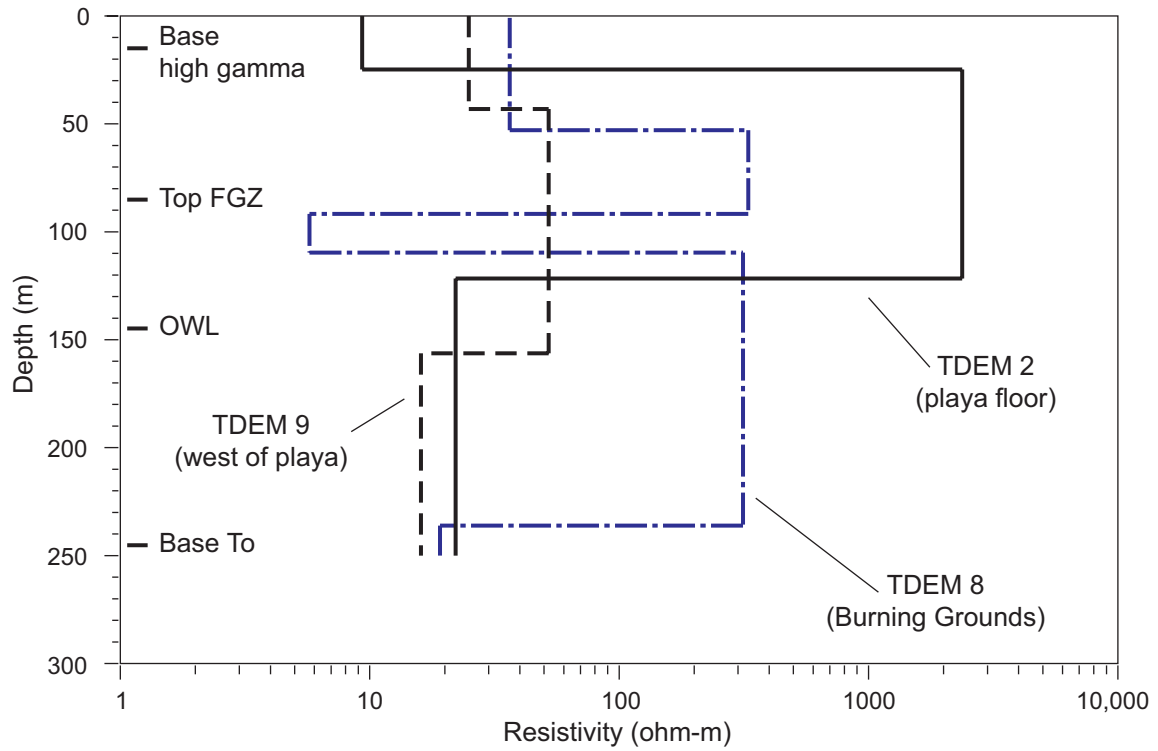


Figure 26. Three- to five-layer resistivity models that fit transients recorded at sites TDEM 2, 8, and 9 in the Playa 3 area. Also shown are the approximate depths to the base of the high-gamma-count zone, the top of the middle Ogallala FGZ, the Ogallala water level (OWL), and the base of the Ogallala Formation (To).



Table 3. Best-fit models for TDEM soundings in the Playa 3 area. Locations on figure 6.

Layer	Resistivity (ohm-m)	Thickness (m)	Conductivity (mS/m)	Depth to top (m)	Depth to base (m)	Elevation at top (m MSL)	Elevation at base (m MSL)
TDEM 2 (Fitting error 1.5 %)							
1	9.3	24.8	107.3	0.0	24.8	1083.2	1058.4
2	2374.3	96.8	0.4	24.8	121.6	1058.4	961.6
3	22.1		45.3	121.6		961.6	
TDEM 8 (Fitting error 1.9 %)							
1	36.5	52.9	27.4	0.0	52.9	1087.5	1034.6
2	329.7	38.8	3.0	52.9	91.7	1034.6	995.8
3	5.7	17.9	174.5	91.7	109.6	995.8	977.9
4	314.1	126.6	3.2	109.6	236.2	977.9	851.3
5	19.1		52.2	236.2		851.3	
TDEM 9 (Fitting error 1.5 %)							
1	24.9	43.1	40.1	0.0	43.1	1086.1	1043.0
2	52.2	113.2	19.2	43.1	156.3	1043.0	929.8
3	16.1		62.3	156.3		929.8	

Southeast and Playa 3. New seismic data would benefit from a more restricted target depth and advances in seismic recording equipment that include greater dynamic range and more recording channels than were available in standard early-1990's equipment.

In the relatively large Pantex Southeast area, where parts of three existing seismic lines provide limited areal coverage, new two-dimensional data could be acquired along multiple lines to provide better definition of the FGZ. These data might be expected to detect the presence or absence, the top, and perhaps the base of the FGZ. More expensive three-dimensional seismic data could be acquired over smaller areas of interest, such as the Playa 3 and Burning Grounds area. These data would be expected to reveal subtle structural and stratigraphic features that distinguish the playa and interplaya environments and influence ground-water migration from the surface to the Ogallala aquifer.

Existing surface and borehole seismic surveys in the Pantex area demonstrate that the natural environment limits the vertical resolution that is readily achievable using seismic methods. Theoretically, the ability of seismic methods to resolve adjacent reflectors is limited to reflectors that are one-fourth to one-eighth of a wavelength apart. Measured seismic velocities of compressional waves within the FGZ are about 1,600 m/s; seismic frequencies above 50 Hz are severely attenuated by the unsaturated and unconsolidated sediments that overlie the FGZ. At these frequencies and velocities, the dominant seismic wavelength is about 32 m. Under the most favorable conditions, seismic resolution within the FGZ is limited to reflectors that are 4 to 8 m apart. This is sufficient to resolve the top and bottom of the FGZ, where it is relatively thick. Where the FGZ thins to less than 4 to 8 m, reflections from the top and bottom of the FGZ will not be resolved but may constructively or destructively interfere in ways that can be analyzed to reveal some thickness information.

Seismic waves with slower velocities, such as shear waves, have shorter wavelengths than compressional waves at the same frequency. Shear waves have been used in seismic surveys to achieve higher resolution than is obtained with compressional waves. Because the FGZ is relatively shallow, a reflection survey that employs a shear wave source might provide better resolu-

tion within the FGZ than a compressional wave survey would. Before a shear-wave seismic survey is conducted, field tests should be conducted to ensure that (a) the FGZ produces shear-wave reflections and (b) what is gained using the slower velocity of shear waves is not offset by lower achievable frequencies.

## TDEM SUMMARY AND RECOMMENDATIONS

In the EM method, we are attempting to exploit the increase in conductivity associated with higher clay and water content within the FGZ to help map the FGZ and estimate its integrity as an aquitard. The approach to establishing whether TDEM provides useful information was to (a) predict the detectability limits of the TDEM method by modeling the perched aquifer and FGZ from existing geophysical logs and (b) prove the viability of the method by acquiring and comparing TDEM soundings at representative locations at the Pantex Plant.

Modeling results using limited resistivity data available from wells at the Pantex Plant suggested that the presence or absence and the thickness of the FGZ are theoretically resolvable assuming that only the FGZ thickness changes. Modeling further showed that a  $100 \times 100$ -m transmitter loop and an 8-ampere current produced a sufficiently strong dipole moment to reach depths greater than that of the FGZ with acceptable signal-to-noise ratios.

Reconnaissance field measurements in the Pantex Southeast and Playa 3 areas showed that these areas are low-EM noise environments that satisfy the lateral homogeneity assumption at most sites. Because the areas have low noise, the TDEM signal arising from depths at and below the FGZ can be distinguished from noise. Because the areas are laterally homogeneous at the scale of measurement, resistivity models can be constructed that reasonably portray generalized resistivity changes with depth beneath the sites.

Transient signals recorded at the 10 reconnaissance sites differ within and between the Pantex Southeast and Playa 3 areas. These differences are caused by changes in the electrical properties of the subsurface in these areas and result in different resistivity models that fit the

observed transients at each site. Although the TDEM method appears to be unable to resolve the thickness of the FGZ, the FGZ does appear to strongly influence the shape of the transient and the resulting resistivity models. The northward increase in FGZ thickness in the Pantex Southeast area manifests itself as a progressive decrease in resistivity in the model layer at the depth of the FGZ. At Playa 3, TDEM data acquired on the playa floor differ greatly from data acquired on the flanks of the playa basin. The playa floor measurements indicate a less resistive (higher clay content) surface layer to a depth of a few tens of meters that is underlain by deposits that are more resistive (coarser or more porous) than those at similar depths on the flanks of the playa. When this information is combined with existing seismic reflection data from the playa, it becomes clear that the stratigraphy beneath the playa probably differs substantially from that in interplaya environments. This is a potential source of error in hydrologic models that assume similar hydraulic properties beneath playa and interplaya settings.

Verification of the accuracy of the TDEM data was hindered by the lack of borehole conductivity or resistivity logs in the areas of interest. These logs should be routinely acquired in future boreholes because they respond well to changes in sediment texture and moisture content.

This study demonstrates that high-quality TDEM data can be acquired at the Pantex Plant, that there is change in the resistivity structure within both areas studied, and that the data are useful in estimating the intensity of FGZ development in the Pantex Southeast area and in examining lithologic differences at depth between playa and interplaya settings. Reconnaissance TDEM data are too widely spaced to provide the spatial density that would be required to map subtle changes in FGZ thickness, FGZ absence in local areas, or channel features within the FGZ. Future TDEM efforts should be directed toward increasing the spatial density of the measurements, either by collecting closely spaced soundings along key transects using ground-based equipment or by acquiring data along closely spaced flight lines using airborne equipment. Key areas where additional TDEM data would be most useful and practical include areas east and north of the main Pantex Plant zones.

## ACKNOWLEDGMENTS

Funding for this study was provided by Sandia National Laboratories under the Innovative Treatment Remediation Demonstration (ITRD) program, P.O. Document No. 12236. We appreciate the efforts of James Phelan and Louise Maffitt of Sandia in support of this study. Pantex staff members Jay Childress, Dale Stout, Mike Keck, Shane Currie, Laura Fox, and C. D. Milford supported field studies at the Pantex Plant. Bureau staff member Andy Graham assisted during the field data acquisition. Lana Dieterich edited the report.

## REFERENCES

- Frischknecht, F. C., Labson, V. F., Spies, B. R., and Anderson, W. L., 1991, Profiling using small sources, *in* Nabighian, M. N., ed., *Electromagnetic methods in applied geophysics — applications, part A and part B*: Tulsa, Society of Exploration Geophysicists, p. 105–270.
- Geonics Limited, 1992, *Protem 47 operating manual*: Mississauga, Ontario, variously paginated.
- Gustavson, T. C., Bebout, D. G., Bennett, P. C., Fish, E. B., Fryar, A. E., Hovorka, S. D., Hua, Hsiao-Peng, Kirschenmann, Kyle, Laun, Scot, Minehardt, T. J., Mullican, W. F., III, Nicot, Jean-Philippe, Paine, J. G., Pezzolesi, T. P., Rainwater, Ken, Ramsey, Heyward, Reedüer, Alan, Romanak, K. D., Scanlon, B. R., Thompson, David, Xiang, Jiannan, Zartman, R. E., 1995, *Summary hydrogeologic assessment, U.S. Department of Energy Pantex Plant, Carson County, Texas*: The University of Texas at Austin, Bureau of Economic Geology, contract report prepared for the U.S. Department of Energy, 127 p.
- Kaufman, A. A., and Keller, G. V., 1983, *Frequency and transient soundings*: Amsterdam, Elsevier, *Methods in Geochemistry and Geophysics*, No. 16, 685 p.
- Paine, J. G., 1992, *1991 Pantex geophysical data acquisition*: The University of Texas at Austin, Bureau of Economic Geology, contract report prepared for U.S. Department of Energy, 24 p.

- Paine, J. G., 1993, Shallow seismic studies of an ephemeral lake (playa) basin on the Southern High Plains, Texas Panhandle: The University of Texas at Austin, Bureau of Economic Geology, final report prepared for U.S. Department of Energy, 37 p.
- Paine, J. G., 1994a, Shallow seismic data acquisition, processing, and interpretation at Playa 3, Pantex Plant, Carson County, Texas: The University of Texas at Austin, Bureau of Economic Geology, final report prepared for U.S. Department of Energy, 32 p.
- Paine, J. G., 1994b, Shallow seismic data acquisition, processing, and interpretation at Pantex Lake, Carson County, Texas: The University of Texas at Austin, Bureau of Economic Geology, report prepared for U.S. Department of Energy, 33 p.
- Paine, J. G., 1994c, Subsidence beneath a playa basin on the Southern High Plains, U.S.A.: evidence from shallow seismic data: Geological Society of America Bulletin, v. 106, p. 233–242.
- Paine, J. G., 1995a, Shallow seismic data acquisition, processing, and interpretation at Playa 5, Carson County, Texas: The University of Texas at Austin, Bureau of Economic Geology, final report prepared for U.S. Department of Energy, 26 p.
- Paine, J. G., 1995b, Shallow-seismic evidence for playa basin development by dissolution-induced subsidence on the Southern High Plains, Texas: The University of Texas at Austin, Bureau of Economic Geology Report of Investigations No. 233, 47 p.
- Parasnis, D. S., 1973, Mining geophysics: Amsterdam, Elsevier, 395 p.
- Spies, B. R., and Frischknecht, F. C., 1991, Electromagnetic sounding, *in* Nabighian, M. N., ed., Electromagnetic methods in applied geophysics — applications, part A and part B: Tulsa, Society of Exploration Geophysicists, p. 285–386.
- U.S. Army Corps of Engineers, Tulsa District, 1992, U.S. Department of Energy Pantex Plant: Amarillo, Texas, hydrogeological assessment, variously paginated.

U.S. Department of Energy, Amarillo Area Office, 2000, Groundwater program management action process: final report prepared by the Environmental Restoration Department, Mason & Hangar Corporation, for the U.S. Department of Energy under subcontract 16189, June 2000, 90 p.

U.S. Department of Energy, Technical Assistance Team, 2000, Protecting the Ogallala aquifer II: recommendations for characterization and remediation of the southeastern plume at the Pantex Plant: final report, July 7, 2000, 21 p.

West, G. F., and Macnae, J. C., 1991, Physics of the electromagnetic induction exploration method, *in* Nabighian, M. N., ed., *Electromagnetic methods in applied geophysics — applications, part A and part B*: Tulsa, Society of Exploration Geophysicists, p. 5–45.